1987-03

Prototype particle size analyzer incorporating variable focal length optics

Kern, Ludwig August

NAVAL POSTGRADUATE SCHOOL
Monterey, California

THESIS

PROTOTYPE PARTICLE SIZE ANALYZER
INCORPORATING
VARIABLE FOCAL LENGTH OPTICS

by

Ludwig August Kern

March 1987

Thesis Advisor Oscar Biblarz

REPORT DOCUMENTATION PAGE

1a REPORT SECURITY CLASSIFICATION: Unclassified	1b RESTRICTIVE MARKINGS
2a SECURITY CLASSIFICATION AUTHORITY	3 DISTRIBUTION/AVAILABILITY OF REPORT: Approved for public release; distribution is unlimited
2b DECLASSIFICATION/DOWNGRADING SCHEDULE	
4 PERFORMING ORGANIZATION REPORT NUMBER(S)	5 MONITORING ORGANIZATION REPORT NUMBER(S)
6a NAME OF PERFORMING ORGANIZATION: Naval Postgraduate School; 6b OFFICE SYMBOL (If applicable): Code 67	7a NAME OF MONITORING ORGANIZATION: Naval Postgraduate School
6c ADDRESS (City, State, and ZIP Code): Monterey, CA 93943-5000	7b ADDRESS (City, State, and ZIP Code): Monterey, CA 93943-5000
8a NAME OF FUNDING/SPONSORING ORGANIZATION; 8b OFFICE SYMBOL (If applicable)	9 PROCUREMENT INSTRUMENT IDENTIFICATION NUMBER
8c ADDRESS (City, State, and ZIP Code)	10 SOURCE OF FUNDING NUMBERS: PROGRAM ELEMENT NO; PROJECT NO; TASK NO; WORK UNIT ACCESSION NO

11 TITLE (Include Security Classification)
PROTOTYPE PARTICLE SIZE ANALYZER INCORPORATING VARIABLE FOCAL LENGTH OPTICS

12 PERSONAL AUTHOR(S)
Kern, Ludwig A.

13a TYPE OF REPORT	13b TIME COVERED FROM ____ TO ____	14 DATE OF REPORT (Year Month Day)	15 PAGE COUNT
Master's Thesis		1987 March	66

16 SUPPLEMENTARY NOTATION

17 COSATI CODES: FIELD	GROUP	SUB GROUP	18 SUBJECT TERMS (Continue on reverse if necessary and identify by block number)
			Particle Sizing; Forward- Scattered-Light Variable-Focal-Length-Optics

19 ABSTRACT (Continue on reverse if necessary and identify by block number)

A prototype particle size analyzer incorporating an innovative variable focal length optical system has been constructed. The device greatly minimizes some particle sizing errors inherent in current analyzers. It also has the advantage of being capable of measuring a wide range of particle diameters inexpensively and accurately.

An existing five lens optical train was modified to allow each lens to be adjusted in three planes and then mounted on a rigid twin rail base to alleviate alignment problems. A precision linear positioning motor was installed to drive a zoom lens that adjusts the system focal length from 1850mm to 5550mm. A photosensor section that measures the intensities of forward scattered light at two different angles was built and evaluated. An analog computer interface has been built into the system to provide the device with automatic and manual control.

20 DISTRIBUTION/AVAILABILITY OF ABSTRACT	21 ABSTRACT SECURITY CLASSIFICATION
☒ UNCLASSIFIED/UNLIMITED ☐ SAME AS RPT ☐ DTIC USERS	Unclassified

22a NAME OF RESPONSIBLE INDIVIDUAL	22b TELEPHONE (Include Area Code)	22c OFFICE SYMBOL
Professor Oscar Biblarz	408-646-2980	Code 67Bi

DD FORM 1473, 84 MAR — 83 APR edition may be used until exhausted. All other editions are obsolete.

19. ABSTRACT (Continued)

During normal automatic operation the computer drives the zoom lens until an optimum intensity ratio is sensed. The system focal length is then determined which yields the corresponding particle size. Successful operation during initial testing has been achieved. Future refinements are suggested.

Approved for public release; distribution is unlimited.

Prototype Particle Size Analyzer Incorporating Variable Focal Length Optics

by

Ludwig August Kern
Lieutenant Commander, United States Navy
B.S., United States Naval Academy, 1975

Submitted in partial fulfillment of the
requirements for the degree of

MASTER OF SCIENCE IN AERONAUTICAL ENGINEERING

from the

NAVAL POSTGRADUATE SCHOOL
March 1987

ABSTRACT

A prototype particle size analyzer incorporating an innovative variable focal length optical system has been constructed. The device greatly minimizes some particle sizing errors inherent in current analyzers. It also has the advantage of being capable of measuring a wide range of particle diameters inexpensively and accurately.

An existing five lens optical train was modified to allow each lens to be adjusted in three planes and then mounted on a rigid twin rail base to alleviate alignment problems. A precision linear positioning motor was installed to drive a zoom lens that adjusts the system focal length from 1850mm to 5550mm. A photosensor section that measures the intensities of forward scattered light at two different angles was built and evaluated. An analog computer interface has been built into the system to provide the device with automatic and manual control.

During normal automatic operation the computer drives the zoom lens until an optimum intensity ratio is sensed. The system focal length is then determined which yields the corresponding particle size. Successful operation during initial testing has been achieved. Future refinements are suggested.

TABLE OF CONTENTS

LIST OF TABLES

LIST OF FIGURES

ACKNOWLEDGEMENTS

The author wishes to express his deepest gratitude to Professor Robert Partelow for endless hours of personal instruction on circuit design and trouble shooting techniques. His everlasting enthusiasm inspired the author's motivation to overcome the most difficult problems presented by this project. The author expresses appreciation to the following individuals: Professor Oscar Biblarz, advisor for this thesis, for his continual interest and support while away on his sabbatical, Professor Sherif Michael for his help with analog integrated circuits, Professor John Powers for his help with photosensors and fiber optics, Professor Crittenden for his help with optics , Professor David Netzer and Professor Jim Miller for their willing advisory assistance. Thank you to Mr. Zeev Shavit for several hours of introductory aid in improving the optical and sensor sections of the device.

A special thanks to Glenn Middleton, John Moulton and Ron Ramaker for their skills in fabricating several system subcomponent assemblies that enabled the project to be successfully completed.

I. INTRODUCTION

The purpose of the overall project is to validate the concept of particle size analysis employing a variable focal length optical system. This device allows the determination of the Sauter Mean Diameter (SMD) of fuel sprays by measuring the intensity of forward scattered light at two angles. When completed the instrument will be capable of measuring a wide range of particle diameters inexpensively and accurately.

The innovative variable focal length optical system is analog computer controlled. It has two advantages over standard fixed focal length systems. First, it allows the optimum intensity ratio to be used for Sauter Mean Diameter determination which reduces sizing errors. Second, it can detect changing particle sizes and provide rate of change information.

Two major areas of interest using particle size analysis are atomizer combustion and pollution studies. This device will facilitate ongoing work at the Naval Postgraduate School investigating spray from turbine engine fuel nozzles and exhaust particles from solid propellent burning rocket engines.

The theory of scattered light particle size measurement on which the analyzer operation is based is presented first. Next comes a general description of each component presently incorporated into the system with mention of the problems that were overcome. Detailed specifics on each component are given in the Appendixes. A brief section on system operation follows. Finally the Conclusions section sums up the successful completion of the prototype analyzer and is followed by further recommendations on improving the present design.

II. THEORY OF PARTICLE MEASUREMENT

The particle sizing method utilized in this thesis is based on the Fraunhoffer principle of forward scattered light. It should be pointed out that the Sauter Mean Diameter (SMD or D_{32}) of a dispersion of particles is what is being measured. The shape of the *tiny* particles is assumed to be spherical.

Three simple statements can sum up the Fraunhoffer principle of forward scattered light.

(1) Small particles scatter collimated light at great angles.

(2) Large particles scatter collimated light at small angles.

(3) Particle diameter size may be directly related to its scatter angle.

A considerably more complete explanation of light scattering by particles written by H. C. Van de Hulst can be found in [Ref. 1].

This principle can be easily demonstrated. If one shines a beam of collimated laser light onto a dispersion of similiar sized particles (mono-dispersion), the light will experience diffraction by the particles to some angle related to size. Light at this diffraction angle is then focused by an objective lens onto a plane at its rear focal point. By placing photodetectors along this focal plane, the corresponding light intensity pattern can be found. The intensity distribution along the focal plane thus becomes simply a function of the particle size, the focal length of the focusing lens and the wavelength of the light [Ref. 2: page 8].

The diagrams in Figure 2.1 show this principle. Note in Figure 2.1(b) how all the light is focused onto the optical axis at the focal plane when no particles are present. Figure 2.1(c) shows how small-size particles scatter light at great angles and will cause an intensity ring far from the optical axis. Figure 2.1(d) shows how large-size particles scatter light at low angles and will cause an intensity ring close to the optical axis.

At each diffraction angle, it is very important to measure only the scattered light. Any extraneous diffracted light will tend to broaden the intensity distribution which in turn would produce additional sizing errors.

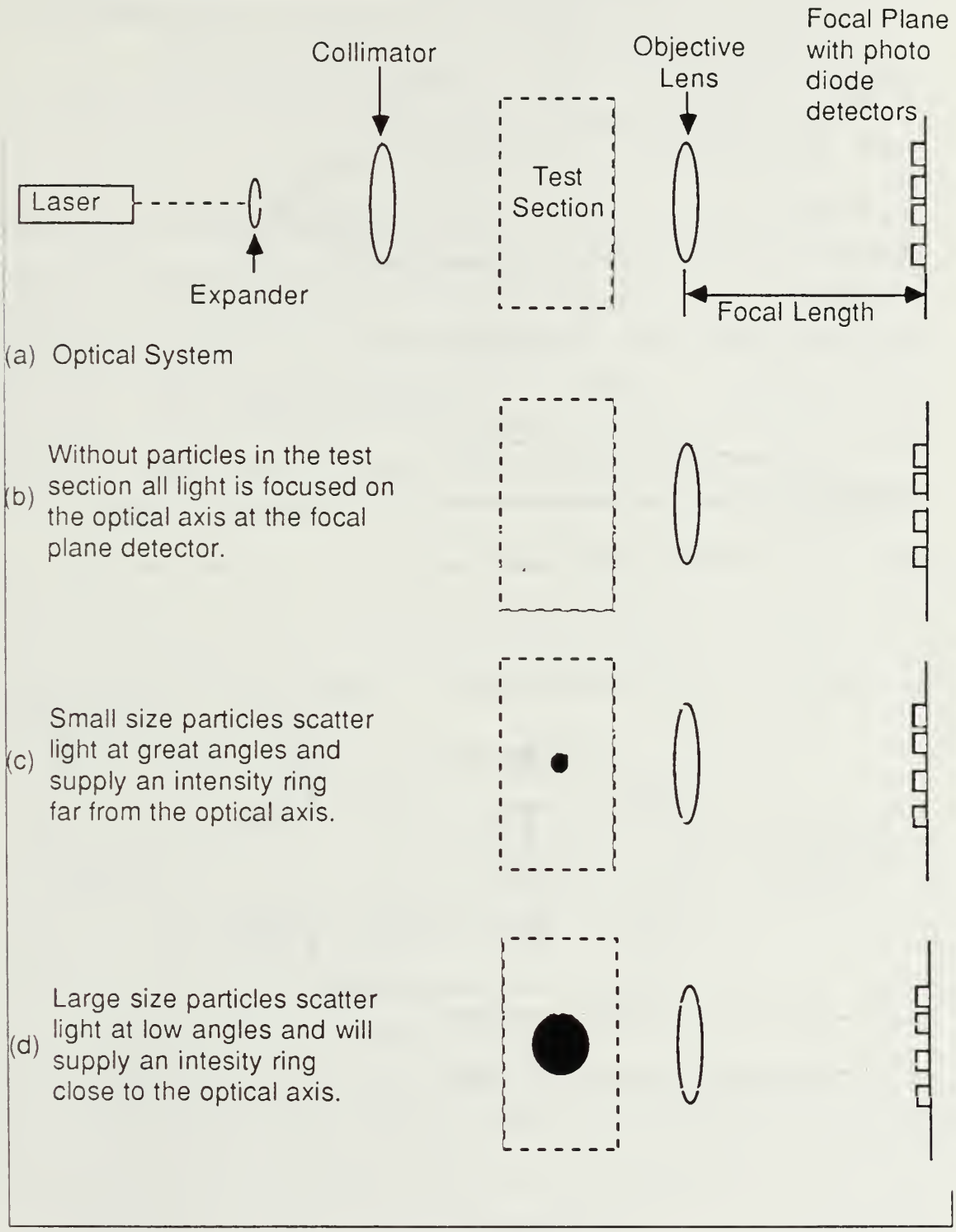

Figure 2.1 Diagrams of scattered light principle.

Some unwanted sources of extraneous diffracted light occur from:

(1) Light beam refraction by air temperature gradients and turbulence,

(2) Scattered light interference between several adjacent particles,

(3) Scattering caused by dirty or imperfect optical surfaces,

(4) Aperture roughnesses about optical components,

(5) Extraneous light in the test section.

Buchelle [Ref. 3] proposes two steps to minimize the effects of this extraneous diffracted light. First, Buchelle says one should use spatially filtered optics. This can be done by introducing a confocal (having the same focal point) pair of lenses (prior to the imaging lens that focuses the scattered light onto the photodetector plane). A beam stop at the common focal point of the confocal pair is required. An additional beam stop at the outer fringe of the imaging lens is desirable as shown in Figure 2.2. Second, Buchelle shows it is desireable to use a *two angle method* of measuring scattered light intensity so that their ratio becomes the important parameter.

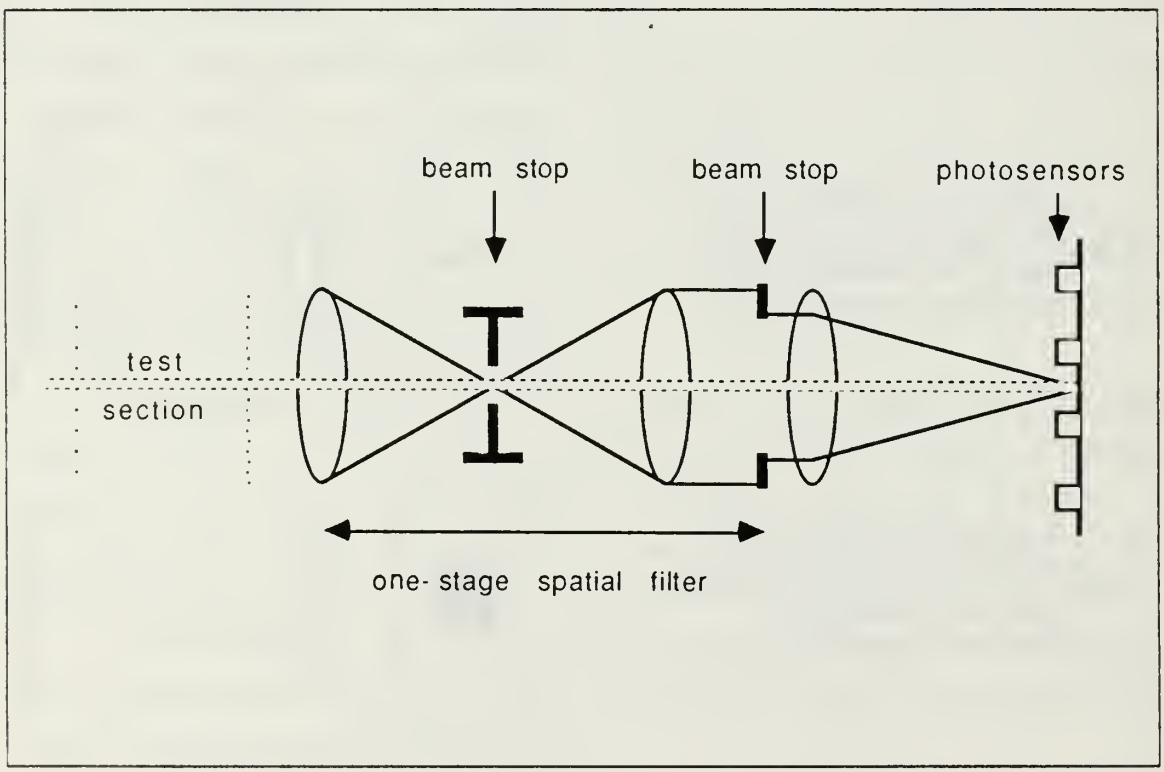

Figure 2.2 Spatial filter.

Assuming a gaussian approximation to the scattering of the diffracted light, Buchelle gives the ratio of intensities at two angles as:

$$I_2 / I_1 = \exp[-(0.57\pi D_{32} \lambda)^2 (\theta_2^2 - \theta_1^2)] \qquad \text{(eqn 2.1)}$$

I_1 = light intensity at θ_1

I_2 = light intensity at θ_2

D_{32} = particle Sauter Mean Diameter

λ = wavelength of laser light source

θ_1 = deflection angle one

θ_2 = deflection angle two

Equation 2.1 shows the desired direct relation between light intensity, wavelength, scatter angle and particle size. The accuracy of this method is based on using the optimum intensity ratio and using two scatter angles as opposed to just one. Buchelle states [Ref. 3] that the uncertainty of this method is less than 5.0 percent for scatter angles less than 0.003 radians.

For small scatter angles the deflection angle can be written as:

$$\theta = y / f \qquad \text{(eqn 2.2)}$$

y = distance from optical axis

f = objective focal length

Figure 2.3 shows how the small scatter angle is approximated by equation 2.2.

Making the substitution for θ from equation 2.2 into equation 2.1 and solving for the Sauter Mean Diameter (D_{32}) yields :

$$D_{32} = (\lambda / 0.57\pi\, y_1)[-\ln(I_2 / I_1)\, [(y_2 / y_1)^2 - 1]]^{1/2} \, (f) \qquad \text{(eqn 2.3)}$$

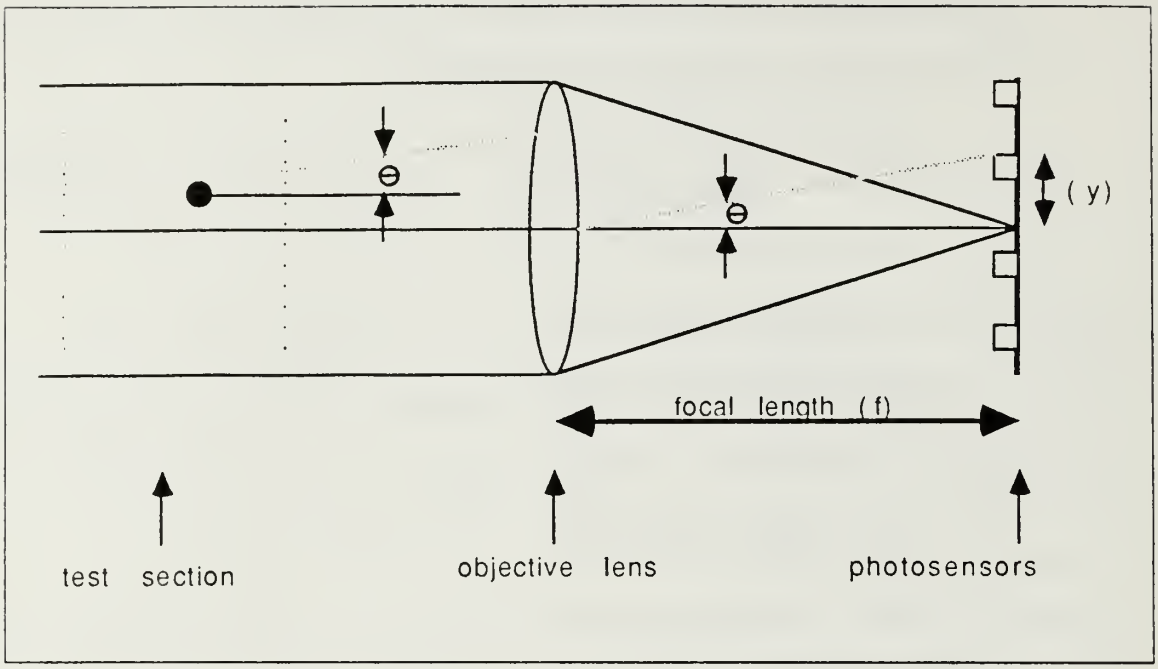

Figure 2.3 Small angle **θ**.

When the laser light wavelength, light intensity ratio, and distances from the optical axis to fixed photodetectors are held constant equation 2.3 becomes:

$$D_{32} = (\text{constant})\, f \qquad \text{(eqn 2.4)}$$

where λ = constant

y_1 = constant

y_2 = constant

$(I_2\ I_1)$ = constant

This is the desired relationship being validated experimentally by the prototype device being developed in this work. Equation 2.4 states that the Sauter Mean Diameter (D_{32}) of a uniform particle dispersion is directly proportional to the optical focal length.

III. PROTOTYPE COMPONENT DEVELOPMENT

The particle sizing apparatus includes a laser light source, test section, optical system, photodetector board with external adjustment disk, automatic control box, manual control box and zoom lens positioning motor with associated cables. This chapter describes the purpose of each component. It also explains the design features used to eliminate optical train alignment difficulties and system noise problems. Specific unwanted noise sources included mechanical vibration, EMI, noisy electronic devices and extraneous diffracted light. Great effort was expended to build the prototype completely modularized. This enables subassemblies within each component to be replaced quickly and easily in case of failure or update improvement.

A. LASER

Laser light is used to approximate an ideal single wavelength DC light source. A 5.0 mW He-Ne laser is presently being used. A "black tube" diffuser which incorporates a beam expander followed by a collimator is mounted to the front of the laser. It diffuses the laser beam 10 times. The conditioned beam leaving this tube has a wavelength of 632.8 nanometers and a beam diameter of 10 millimeters. The laser is shown in Figure 3.1.

B. TEST SECTION

The test section is the region where the particles to be measured actually do their light scattering. The device can be set up to accomodate numerous test sections. The test section location must allow the optical system to be at least 6.5 feet away. The reason for this limitation is because the optical system is focused at infinity which is considered to be three first-objective-lens focal lengths away.

The device is currently set up about a liquid fuel spray nozzle which can remain open to the atmosphere. This configuration minimizes light refraction errors that occur when windows or pressure boundries exit about the test section. Figure 3.1 shows the test section during device alignment.

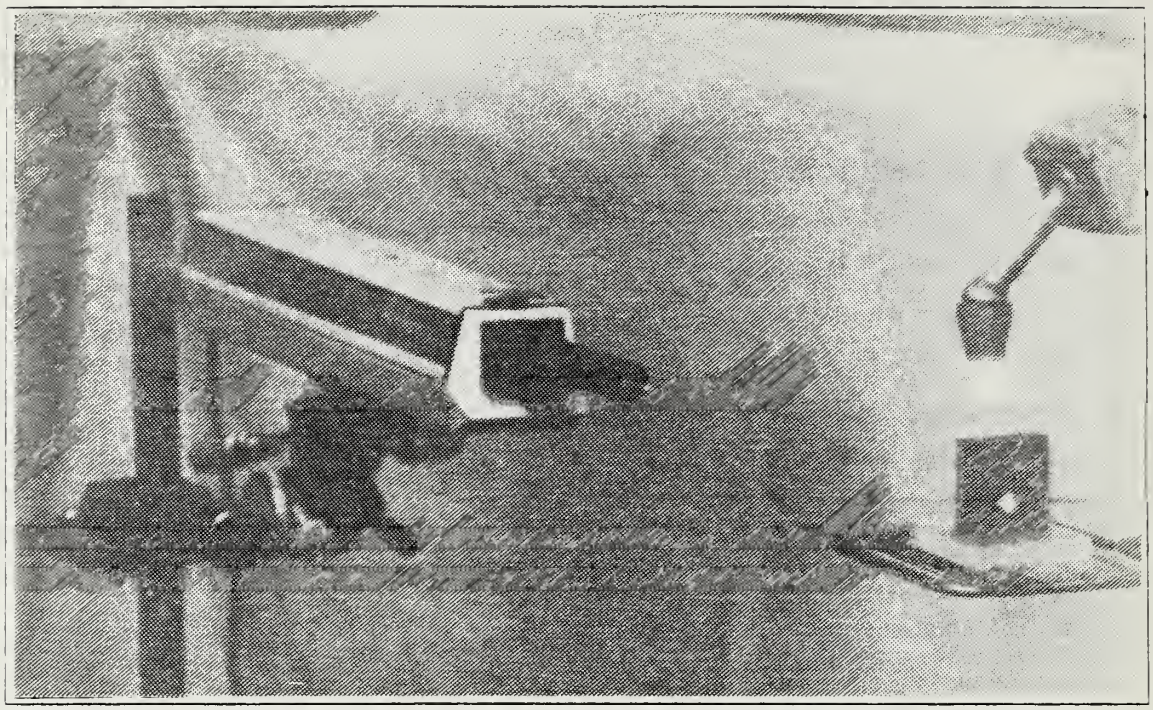

Figure 3.1 Laser source and test section.

C. OPTICAL SYSTEM

At the heart of the system is a five-lens train originally conceived and assembled by John Powers [Ref. 4]. His carefully devised scheme sets up the first four lenses in two confocal pairs. Each confocal pair acts as a spatial filter to attenuate extraneous diffracted light. This is intended to minimize error. The fifth lens focuses the conditioned scattered light onto the photodetector plane. These five lenses were originally mounted on a single optical rail and aligned with the laser.

An innovative idea by Donald Buchelle [Ref. 3] for incorporating a zoom lens into a spatial filter has been adopted and expanded upon. The zoom lens varies the effective focal length of the system. This enables one to fix the optimum intensity ratio and allow the system to focus until it is actually reached. A commercial Vivitar zoom lens (70mm to 210mm) has been incorporated into the spatial filter. It allows the system focal length to be changed from 1850mm to 5550mm. The zoom lens is physically shown in Figure 3.2 as lens (3).

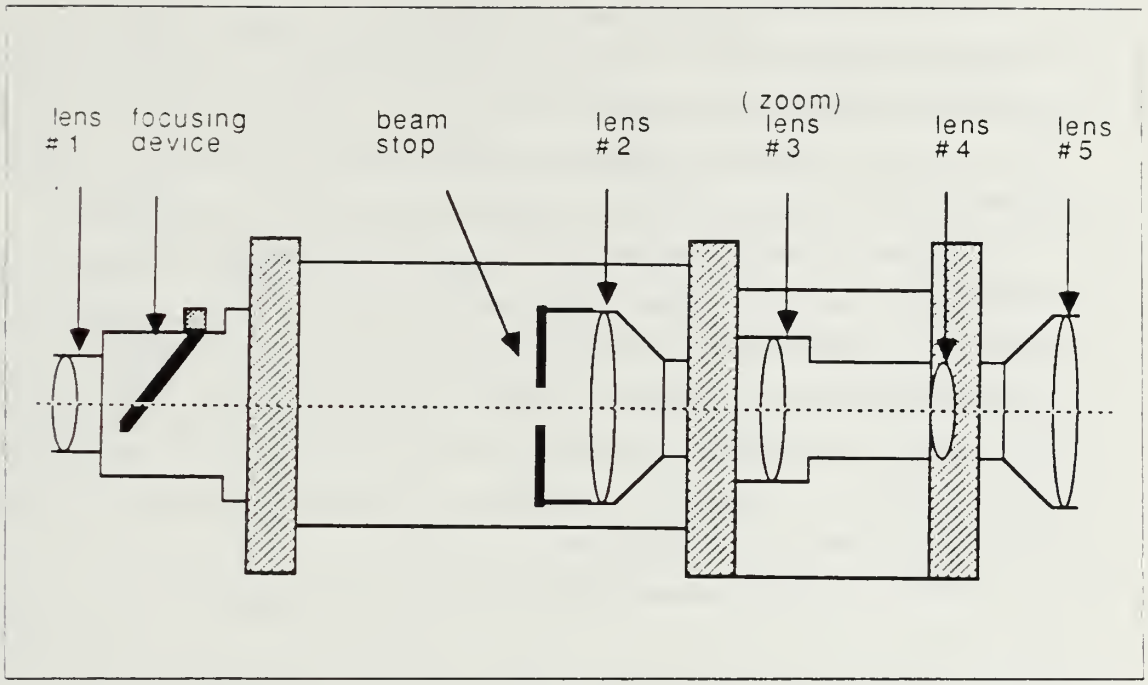

Figure 3.2 Lens configuration.

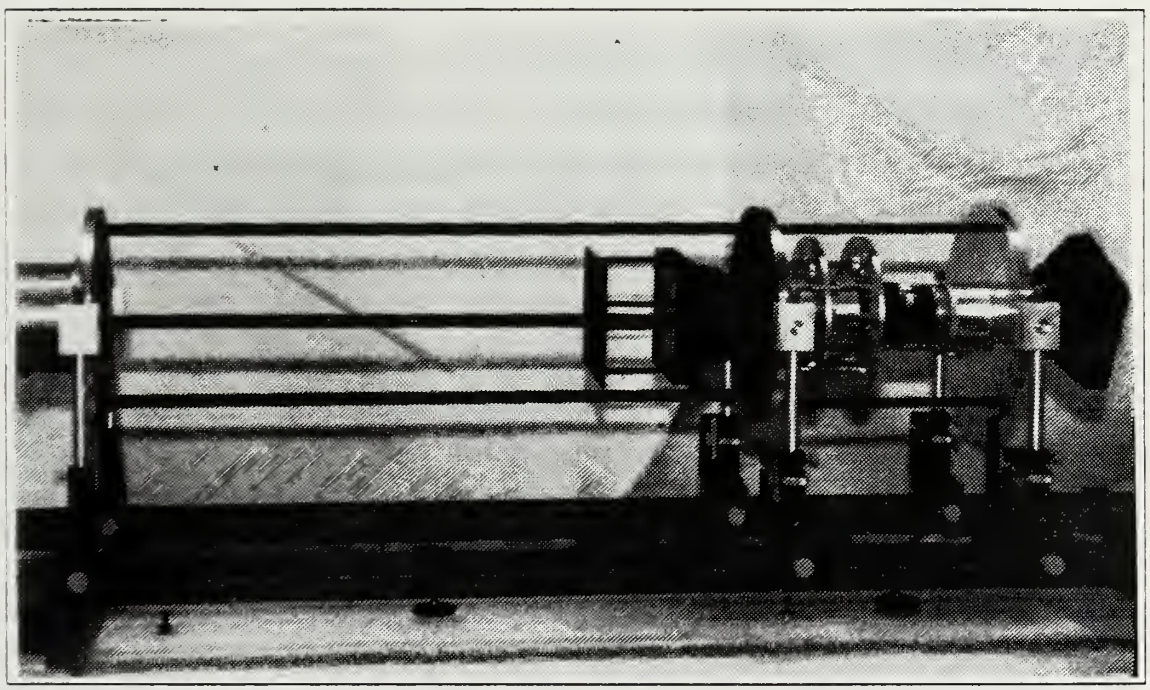

Figure 3.3 Actual system optical train.

Zeev Shavit [Ref. 2] found initial alignment of the original five lens system (which requires a tolerance within a fraction of a radian) very difficult. It took several hours of minute adjusting to reach an acceptable alignment. Unfortunately as soon as the zoom lens positioning motor was engaged the optical system would wobble due to induced vibration. As the system wobbled it would oscillate in and out of alignment.

Two improvements were made to ease the initial alignment problem. First an objective lens adjusting device similiar to one used on a 35mm camera lens and suggested by Shavit [Ref. 2] was incorporated. It enables the first objective lens to be easily moved forward and back with a 4.0-inch travel. This allows its focal point to be focused onto the forward focal point of lens (2) within seconds. Next, a new optical mounting system was designed and installed to give both a horizontal and vertical adjustment to lenses (2),(3),(4) and (5).

In order to alleviate system wobble while the positioning motor was running, two sets of legs were manufactured for a double optical rail base configuration. One set of legs is attached to each side of the optical support disks. This reduces the degrees of freedom of movement available to the system. A smaller, quieter motor was also installed. These two improvements were suggested by Shavit [Ref. 2].

Specific details and designs with incorporated improvements of the present optical system are included in Appendix A.

D. PHOTODETECTOR SYSTEM

The development of an acceptably low noise photodetector system was the most exacting task of this thesis.

First, a scheme taking each photodiode output voltage and running it through a series of external 741-operational amplifiers was built and tested. This was done to complete work originated by John Powers [Ref. 4.] This configuration proved to be very noisy at low photodiode input voltages. This is because the 741-operational amplifiers become voltage sources themselves when input voltages approach zero. Selecting a FET-type operational amplifier equivalent to the 741 alleviated this problem.

A photodetector made by EG&G classified as the HAD-1100A incorporates a high gain FET amplifier with a photodiode in a single package. A breadboard circuit using this photodetector was constructed for comparison testing. The circuit provided a very low noise output. It also provided sufficient gain with its single internal amplifier which eliminated the need for several amplifier stages.

A hardwired photodetector board was constructed which allows room for four HAD-1100s. The four photodetectors are arranged in a single line so that they are able to sense scattered light intensity at four different distances from the optical axis. Each photodetector converts the light intensity it senses into a voltage.

Each voltage is output from the board to the photodetector external adjustment disk at the rear of the device. The disk has connections for each detector voltage to be simultaneously monitored on an oscilliscope. It contains the offset adjustment for each detector amplifier. These controls allow the photodetector outputs to be easily set to zero when there are no particles in the test section. The disk also incorporates the photodetector selector switch which determines which pair of detector output intensity voltages will be sent to the automatic control box. A rod that can slide through the disk serves as a support for the photodetector board. The rod slides so that the photodetector board can be adjusted until its position coincides with the focal plane of the last lens.

Pictures, schematics and specific details of the photodetector board are found in Appendix B. Similar information on the photodetector external adjustment disk is found in Appendix C.

E. AUTOMATIC CONTROL BOX

The capability for automatic system operation was a high design priority for the prototype device. An initial scheme [Ref. 4] incorporating an automic control circuit inside the rear sensor cavity with the photodetector board proved unsuitable. It was too difficult to monitor and adjust by requiring the operator to remove the sensor section light shielding each time. The lessons learned resulted in the design of a dedicated automatic control box with a simple external capability for inputing optimum reference intensity ratios into the system.

The automatic control box supplies an analog signal that is automatically computed to drive the positioning motor until the zoom lens is positioned correctly. Inside the automatic control box is an analog computer card. It compares the actual intensity ratio sensed by the selected pair of photodetectors to the optimum reference intensity ratio. The reference intensity ratio is input by the operator by adjusting a 10-turn potentiometer on the top of the box. The card output is a conditioned error signal between the actual and reference intensity ratios. It is conditioned to give a + 10 volt DC signal for positive errors and a -10 DC volt signal when it senses negative

errors. These voltage values were selected because they are the maximum voltages the positioning motor has been built to accept. This logic allows the system to position the zoom lens in minimum time.

Monitoring jacks on the front of the automatic control box allow a digital multimeter to be conviently hooked up. This enables the operator to easily verify computer card operation via digital readout without opening the box. An AUTO MANUAL switch is also located on the top of the box to allow the automatic mode to be bypassed during initial system calibration.

Specific details including analog circuit logic, wiring schematics and color codes are given in Appendix D.

F. MANUAL CONTROL BOX

The need for system calibration and verification dictates a requirement for a manual control mode for positing the zoom lens. A commercial manual control box was purchased which met this need with the additional desired feature of a digital readout.

Previous system output was given in the form of an analog strip chart trace from a pen recorder. With the incorporation of the digital readout into the system, the zoom lens travel is now a direct readout available in both manual and automatic modes of operation. Several series and parallel interface connections between the manual and automatic control boxes were necessary to make the system work. These connections are described in Appendix D.

The specific details including a picture of the manual control box are included in Appendix E.

G. POSITIONING MOTOR

Initially [Ref. 4] the system was driven by a large 28 volt DC servo motor which turned a micrometer screw via a five gear train to position the zoom lens. Unfortunately the gear train induced too much error into the system due to backlash. Also, the motor itself produced such great vibration that it caused both optical misalignment and mechanical noise problems to an unacceptable degree.

An extensive search for a precision linear positioning motor that would fit into the already assembled hardware provided only one candidate motor. It is the commercial 850-1 positioner sold by Newport Corporation. This motor has its own micrometer screw plunger and is mated to the device. It provides much more accurate

positioning with an undetectable level of mechanical vibration. Details about the positioning motor are included in Appendix F.

H. OTHER COMPONENT CONSIDERATIONS.

To reduce system noise from EMI sources, a substantial amount of wire shielding has been incorporated into the photodetector cavity and automatic control box. The external ribbon interconnect cables that came with the motor are not shielded and may still pose a problem. If further test and evaluation proves that their shielding is required, commercial shielded ribbon cables are available for the system from Newport Corporation. Specific details about the ribbon interconnect cables are given in Appendix G.

Beamstops are used to eliminate optical noise. Presently only one beamstop is employed in the system. It is a single slit located at the co-focal point between the first and second lenses as previously shown in Figure 3.3. A 2.0-millimeter wide center block is installed across the slit during normal operation which prevents unscattered light from continuing through the device. This arrangement allows only a small sample of scattered light to pass through the slit on both sides of the center block. The line of photodetectors at the rear of the device is positioned so its orientation matches that of the beamstop slit.

An additional trial beamstop comprised of five pinholes was installed [Ref. 4] at the confocal point between the third and fourth lenses. The pinholes, 50 microns in diameter, were placed in a horizontal line. The center pinhole allows unscattered light to pass through the optical axis of the system during alignment. The other four pinholes allow scattered light to pass through to the four photodetectors. The theory behind using pinholes at this stop was to ensure scattered light would only be permitted to pass through at predetermined distances from the optical axis. This would minimize the position error associated with the location of each photodetector and its distance (y_1 or y_2) from the optical axis. Unforntunately the system would not work with this second beamstop installed so it was removed. Future testing with larger pinholes is desirable and is described later in the recommendations portion of this report.

IV. PROTOTYPE OPERTATION

Several operational tests have been successfully completed on the analyzer. This chapter will discuss the three phases of operational testing that were performed.

First, tests in the manual mode were performed which concentrated on alignment maintainability and optical system calibration. For this phase the new adjustment capability for each lens worked perfectly. The 1.0-cm. diameter laser beam was easily focused to a 300 micron dot precisely at the confocal point between lens (1) and (2). This step which previously took more than an hour of adjusting was completed within seconds by the new first objective focusing device. The remaing four lenses were adjusted until the laser beam was boresighted on the photosensor board at the focal plane of lens (5).

With the system roughly aligned, the zoom lens (lens 3) was driven forward and aft with the positioning motor in the manual mode. No system wobble or vibration was detectable but the laser dot (reticle) that had been previously boresighted drifted to the left 1.2-cm. as the zoom lens moved forward. It returned to boresight when the zoom lens was moved back to its original position. Fortunately, this problem was easily rectified with a few more horizontal adjustments of lens mounting disks (2) and (3). These adjustments positioned the zoom lens cylinder axis (which had been slightly canted) into perfect alignment with the optical axis. With the system now remaining boresighted during manual zoom lens positioning, the set screws were firmly tightened to lock the lens components into position.

System portability was also taken into consideration. The device was moved to a new location and the laser was aligned through the first objective lens without unlocking any set screws. The zoom lens was then manually driven forward and aft with only a two millimeter horizontal deflection. Although several reasons for this slight movement are possible, the result of this test proves the prototype can be repositioned without requiring major realignment adjustments.

The final portion of manual mode testing compared the actual travel of the zoom lens with the digital position readout on the manual control box. The position readout did an excellent job of presenting accurate zoom lens displacement. An important operating procedure was also gained during the test. This procedure calls for the

operator to return the zoom lens all the way to its 30mm position and then initialize the digital display to zero. This is necessary because the display has no memory and reads zero each time the system power is turned on. If the zoom lens were already extended when power is supplied the readout on the display will be incorrect. A list of system operating proceedures is included in Appendix H.

Analyzer open-loop operation was investigated during the second phase of experimental testing. This phase concentrated on the photosensor section and analog computer operation in which both performed correctly.

Initial photosensor testing was done using attenuated *unscattered* laser light. The noise to signal ratio of each photodetector was checked over a range of gains from 10 to 1000. A very low noise to signal ratio of (.02 to .04) was found. An artificial light intensity ratio was produced in the photosensor section by setting a different gain between each detector. This was done to produce simulated actual intensity ratios between (.50) and (.85) for the analog computer computation. The output from each detector was continuously monitored via oscilloscope for correlation during these tests.

The analog computer properly received the intensity voltages and computed the actual intensity ratio for each pair of detectors selected. These ratios were checked by monitoring the intensity ratio error signal on the automatic control box with the reference intensity ratio set to zero. The next step in this test required the computer to computed the correct error between the actual and reference intensity ratios. As expected, each time the input reference intensity ratio was adjusted until it matched the actual intensity ratio, the output error went to zero.

Next, the amplifier logic section was checked to determine if the computer actually functions as the motor preamplifier. It was successful in providing -10 volts DC when the error was negative, +10 volts DC when the error was positive and less than a half volt DC when the error was zero.

With the system fully functioning in this open-loop mode several tests were made using the computer to drive the zoom-lens positioning motor. In these tests the actual photodetector intensity ratio was held constant while the reference intensity ratio was adjusted until their corresponding error was zero. (NOTE: This is just the opposite of what happens in the normal closed-loop operation where the reference intensity ratio remains fixed and the actual intensity ratio is adjusted with zoom lens position.) Successful computer control of the positioning motor was achieved. The motor moved the lens forward when the error signal was negative and backward when the error

signal was positive. It stopped when a zero error signal was reached and the "yellow" limit light illuminated on the manual control box.

The third phase of experimental testing investigated automatic closed-loop operation of the particle size analyzer. These tests concentrated on the system's ability to automatically drive the zoom lens to the null position.

For closed loop operation all of the HAD-1100A detectors had their gains matched at 100. With the laser turned on and the test section empty, the output of each detector was initialized to zero with the corresponding offset adjust. An optimum reference intensity ratio of (.70) was input into the computer. The test particles for these experiments were liquid aerosol droplets from a commercial aerosol spray can. The outer pair of photodetectors was selected corresponding to the 17μm-90μm size range.

As spray into the test section commenced, the intensities from detectors (1) and (4) were monitored on the ocsilloscope. Their intensities immediately increased from zero to approximately 2.8 and 2.4 volts respectively, with a peak to peak noise value of .30 volts each. This yielded the first data on the intensity of scattered light each photodetector senses prior to amplification. Dividing these detector outputs by their gain of 100 yields photodiode intensities of 28mV and 24mV.

While allowing the spray to continue through the test section, the AUTO mode was selected on the automatic control box. The computer successfully drove the positioning motor to a null. At this null position the intensities monitored on the oscilloscope from detectors (1) and (4) had changed to 3.0 and 2.1 volts respectively. This results in an actual intensity ratio [$\text{intensity}_{(4)}$ $\text{intensity}_{(1)}$] of (.70) which confirmed zero error with the chosen reference intensity ratio.

A D_{32} size of 52μm was computed for the aerosol spray based on a zoom lens linear position of 7.2mm. Procedures used for D_{32} determination can be found in Appendix H.

V. CONCLUSIONS

Several new components have been successfully incorporated into the prototype variable focal length particle size analyzer. Alignment problems have been eliminated by three new design features: an individual focusing device for the first objective lens, a twin optical rail base to maintain optical system rigidity during operation, and six piece optical legs that allow the lenses to be easily adjusted horizontally and vertically.

Two sources of system noise have been practically eliminated. Mechanical vibration is no longer detectable with the new linear positioning motor installed. Electrical noise has been greatly reduced by the new photodetector system. It is believed that optical noise can be further reduced by incorporating optimum beamstops. Work on the beamstops should continue.

An automatic mode of operation has been built into the system and has worked successfully under simulated conditions. System output via digital readout is now available. The theoretical range of particle sizes to be measured by the prototype has been expanded to 12.6μm - 266.0μm.

The variable focal length particle size analyzer is ready for future evaluation with standard sized particles. There is confidence that this prototype can be developed into a useful laboratory tool.

VI. RECOMMENDATIONS

Full scale test and evaluation of the device using standard size particles should be the next step taken. It would be beneficial to test particles in each selectable range. Perhaps 20μm, 50μm, and 150μm could be tested. Results from these tests should provide enough data for an initial error analysis. It is necessary to establish a baseline system error as soon as possible. This will allow future improvements to be rated on their ability to reduce error. In this way some future-improvement options might prove *unneccessary* because of their minimal effect on error. They could even end up increasing system error which is a possibility that should not be overlooked.

The error induced by unmatched photodetector amplifiers is one area that should be analyzed this way. The gain of each amplifier is presently set by pluging a pair of fixed resistors for each HAD-1100A into a bank of sockets. This is an easy configuration to change each amplifier's gain quickly from 100 to 1000 by simply replacing each feedback resistor with one of 10 times higher resistance. Unfortunately they would probably be no longer perfectly matched. Their new gains could easily range from 950 to 1,050 with the 5.0% resistors presently To eliminate this problem high precision resistors should be used. Using 1.0% resistors would improve the gain range in the previous example to 990 to 1010. Resistors with a 0.1% tolerance would even be better but expensive.

Optical error that can be eliminated by better beamstops is another area that should be futher investigated. Variable slit size knife-edge beamstops can be easily found for incorporation into the system as beamstop number one. The optimum slit size setting can be determined through system testing with standard sized particles to find out what setting gives the least error. A second beamstop should be installed at the confocal point between lenses (3) and (4). A simple slit could be tried first. If this proves acceptable, large size pinholes (500μm) could be placed along the slit at the optical axis and at the corresponding distance for each photodiode. These critical distances must be calculated using optical lens magnification equations and the corresponding photodiode spacing given in Appendix B. If the pinholes on the second beamstop still prove unacceptable, then a third beamstop placement option right in front of the detectors may be possible. This third beamstop would have to be located

a the focal plane of the last lens and could contain the 500μm pinholes previously mentioned. Again, the neccessity of this third beamstop should be determined experimentally based on its ability to reduce system error.

Optical error might also be reduced by incorporating a beam chopper between the test section and the first objective lens. A wide range of chopper frequencies should be analyzed experimentally to determine their effects on noise reduction.

The system needs to be mounted on a vibration isolated optical table. The laboratory table presently used does not provide adequate support nor vibration isolation. Commercial tables available for holographic experiments should suffice.

The system would be greatly enhanced as a laboratory tool if the present automatic control box was replaced by a digital computer with a display. This would allow the user to make system inputs via keyboard and receive output in graphical or tabular form. The present positioning servo-control is completely digital compatible.

Future device capability may be greatly expanded by replacing the four photodetector array with a 1024-photodiode digitally sampled linear array. Such an array has already been acquired for the device but would require the previously mentioned digital computer interface to be installed first.

APPENDIX A
THE OPTICAL SYSTEM

1. LENS DATA

The five lenses used were chosen on the basis of minimum cost and availability. As a result only minor attention was paid to the quality of the optical elements employed. Nevertheless, a satisfactory optical resolution has resulted [Ref. 2]. Specific lens data are shown in Table 1.

TABLE 1
LENS DATA

Lens	1st Lens	2nd Lens	3rd Lens	4th Lens	5th Lens
Origin	Opaque Projector	Aerial Photo Camera	Vivitar Series One	Closed Circuit TV Camera	Aerial Photo Camera
Type	Convex	Aspheric	Convex	Convex	Aspheric
Focal Length	660.4 mm (26.0 in)	152.4 mm (6.0 in)	70-120 mm (2.8-8.3 in)	25.0 mm (0.98 in)	152.4 mm (6.0 in)
Aperture Diameter	101.6 mm (4.0 in)	23.4 mm (0.93 in)	20.0 mm (0.79 in)	17.9 mm (0.70 in)	23.4mm (0.93 in)
f number	6.5	6.5	Variable	1.4	6.5

The zoom lens has been prefocused to infinity. This position is used to give the least optical distortion. As a result, the particle test section must be at a great enough distance from the the optical train to meet the infinite distance requirement. A distance of three times the first objective focal length [i.e., 198 cm. (78 in.)] meets this criterion.

2. SYSTEM FOCAL LENGTH

The focal length of the entire optical train is determined by the specific five lens configuration shown in Figure A.1 on the following page. In this arrangement the focal length of the system is given as [Ref. 4: page 19]:

$$f_{system} = [f_1 f_2] [f_3/f_4] f_5 \qquad \text{(eqn A.1)}$$

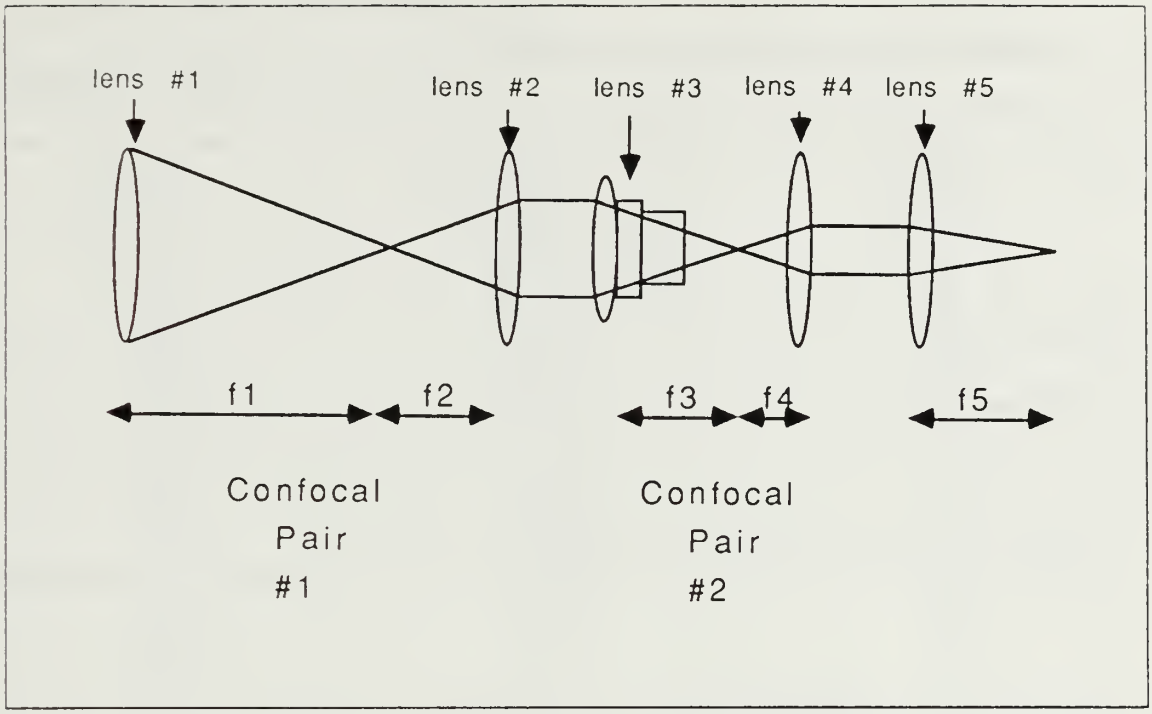

Figure A.1 Lens train configuration.

For the known constant focal lengths this becomes:

f_{system} = [660.4mm 152.4mm] [f_3 25.0mm] 152.4mm

Finally:

f_{system} = 26.4 (f_3) in millimeters (eqn A.2)

The only unknown variable in equation A.2 is (f_3). It is the zoom lens focal length which is determined by the linear position of the zoom lens housing. A digital readout gives the position of the zoom lens in millimeters. Table 2 gives the correlation between zoom lens linear position and system focal length. From the table, one can see that a digital readout of a 0.0 mm linear position corresponds to a 210.0 mm focal length and a 31.0 mm linear position corresponds to a 70.0 mm focal length. These are the physical limits of the zoom lens.

TABLE 2

SYSTEM FOCAL LENGTH CORRESPONDING TO ZOOM LENS TRAVEL

Zoom Lens Travel (mm)	Zoom Lens Focal Length (f_2) (mm)	System Focal Length (mm)
0	210.11	5547
1	205.48	5428
2	200.97	5309
3	196.45	5189
4	191.94	5070
5	187.42	4951
6	182.90	4832
7	178.38	4712
8	173.87	4593
9	169.35	4474
10	164.84	4354
11	160.32	4235
12	155.81	4118
13	151.29	3996
14	146.77	3877
15	142.26	3758
16	137.74	3639
17	133.23	3519
18	128.71	3340
19	124.19	3281
20	119.68	3161
21	115.16	3042
22	110.65	2923
23	106.13	2804
24	101.61	2684
25	97.10	2565
26	92.58	2446
27	88.06	2326
28	83.55	2207
29	79.03	2088
30	74.52	1968
31	70.00	1849
Total Range 31 (mm)	Total Range 140 (mm)	Total Range 3698 (mm)

As mentioned in Appendix F, the positioning motor plunger has a maximum travel range of only 27.5 millimeters. To make full use of the 31.0 millimeter range of the zoom lens, the motor can be adjusted forward and the digital readout can be calibrated to read 2.5 millimeters initially. The plunger can then move the zoom lens out to its full range of 31.0 millimeters.

3. LENS MOUNTING DISKS

The five lens elements are mounted on three parallel aluminum disks. Each disk is .500 inch thick with a 9.875 inch diameter. The disks are held rigidly parallel by two sets of three .500 inch-diameter steel rods. These rods are bolted to the outer edges of each disk at even intervals, 120 degrees apart. Each disk also has a center hole large enough to allow the desired light to pass through it.

The exact spacing between the lens mounting disks is critical. The spacing between disk one and two must ensure lenses (1) and (2) have a common focal point [i.e. the aft focal point of lens (1) coinsides with the forward focal point of lens (2)]. Similarly, the spacing between disk two and three must ensure lens (3) and lens (4) have a common focal point. Each associated set of steel rods have been precision made in length to provide the critical spacing required. The length of each rod between disk one and two is 73.0 cm. (28 3/4 in.). The length of each rod between disk two and three is 25.2 cm. (9 15/16 in.).

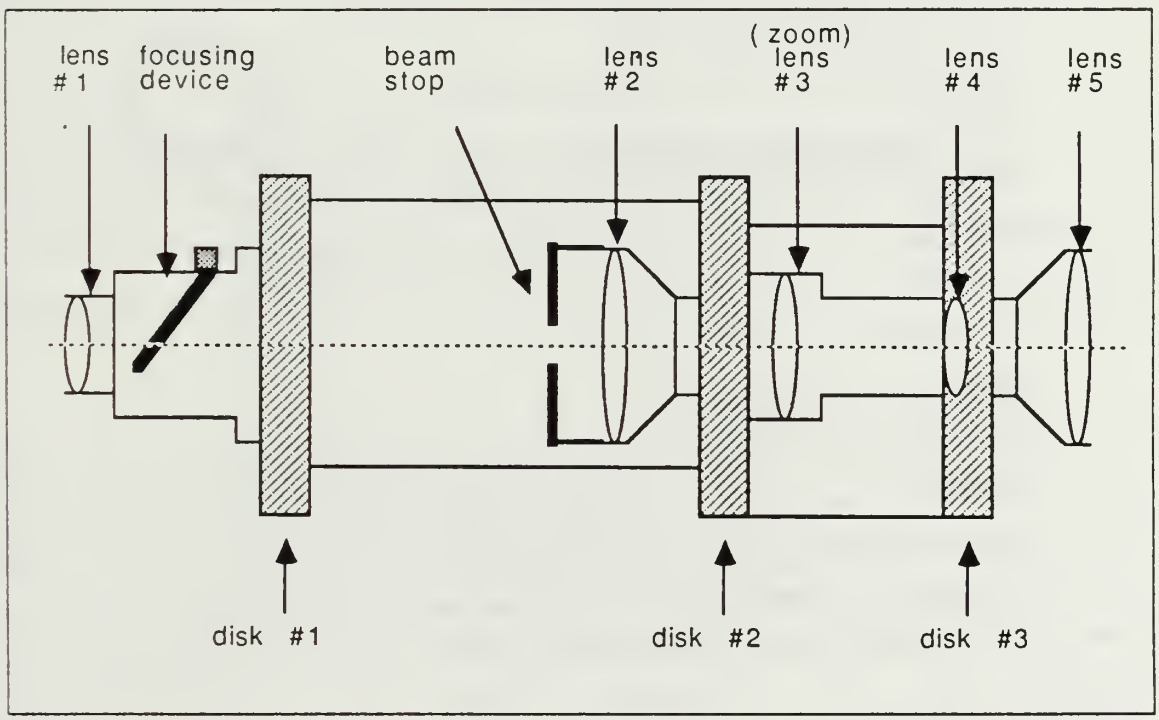

Figure A.2 Optical lens and mounting disk configuration.

The overall mounting disk and lens configuration is shown in Figure A.2 . Disk one has the first objective lens and its associated adjusting device mounted on its

forward face. Disk two supports a beamstop followed by lens (2) on its forward face and zoom lens (3) on its aft face. Disk three also supports the zoom lens, but on its forward face. It has an internal mounting for lens (4) and supports lens (5) on its aft face.

4. OBJECTIVE LENS FOCUSING DEVICE

A two piece focusing device was designed and installed to ease the initial alignment step. Its specific purpose is to adjust the aft focal point of the first objective lens so it coincides perfectly with the forward focal point of lens (2) at the first beamstop.

The inner piece of the device is an aluminum sleeve that acts as the moveable objective lens holder. The outer piece is made of brass. It serves as the fixed outer housing. This outer housing has a 40 degree leading groove that enables the lens to be adjusted exactly 4.0 inches laterally. A set screw is incorporated into the housing to lock the lens into the desired position. The first objective lens focusing device is shown in Figure A.3 .

5. OPTICAL SYSTEM MOUNTING LEGS

The optical system is supported by a total of six aluminum mounting legs. A pair of legs is attached to each lens mounting disk (one leg on each side). The legs were especially designed to maximize rigidity while allowing lens adjustment in two planes. A five piece assembly is required for each leg. Figure A.4 the design and dimensions of the complete assembly for a single leg.

6. OPTICAL MOUNTING FEET

Six aluminum mounting feet secure the six mounting leg assemblies to the optical rails. The two feet that attach to the mounting legs of disk one of the system are of the usual fixed configuration. The remaining four feet are specially designed to enable vertical adjustment of their associated mounting legs. This feature allows the last two lens mounting disks to be individually precision adjusted in their vertical planes. These mounting feet were commercially purchased from Physitec Corporation (Ph 617-528-4100).

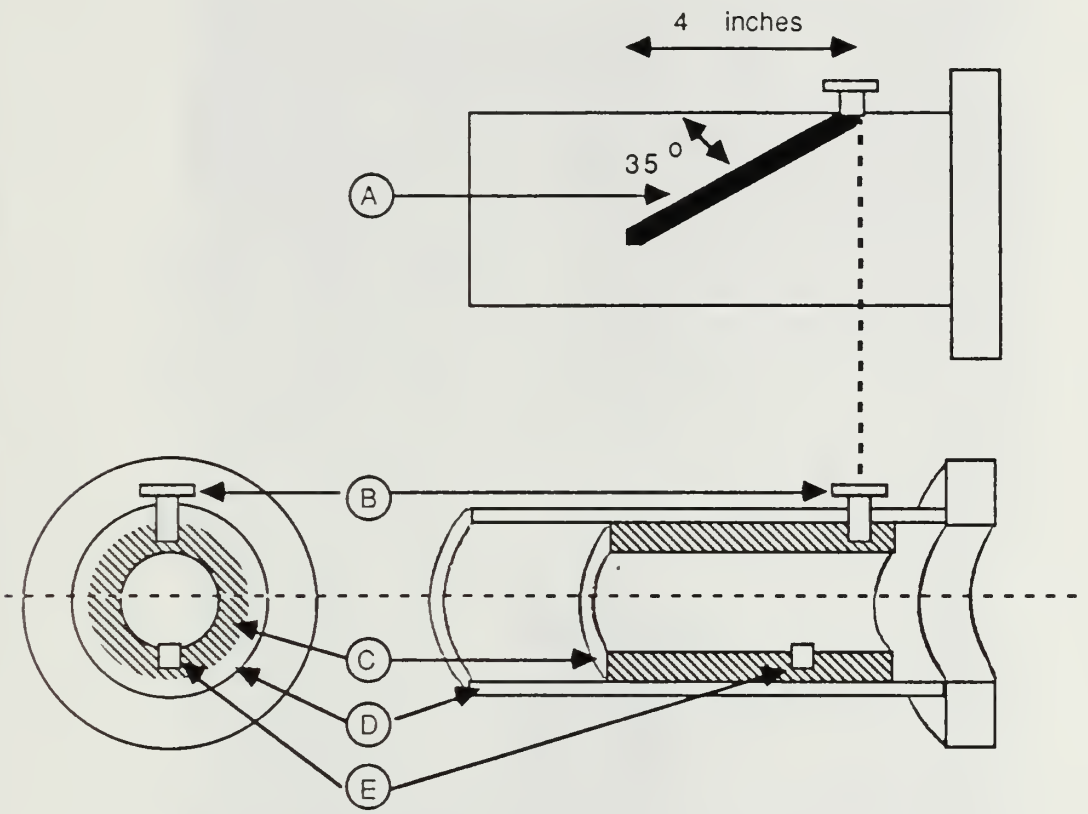

(A) Leading Groove
(B) Screw Drive
(C) Moveable Lens Holder
(D) Fixed Outer Housing
(E) Plastic Set Screw

Figure A.3 First objective lens focusing device.

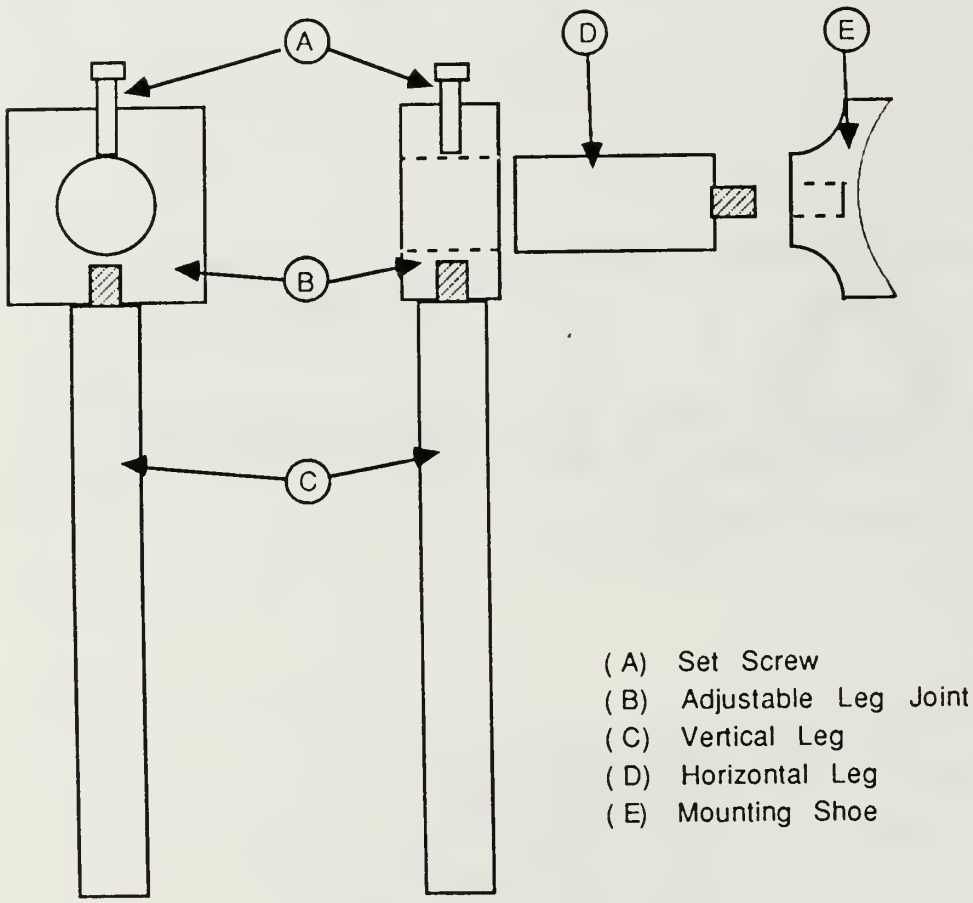

Figure A.4 Optical system mounting legs.

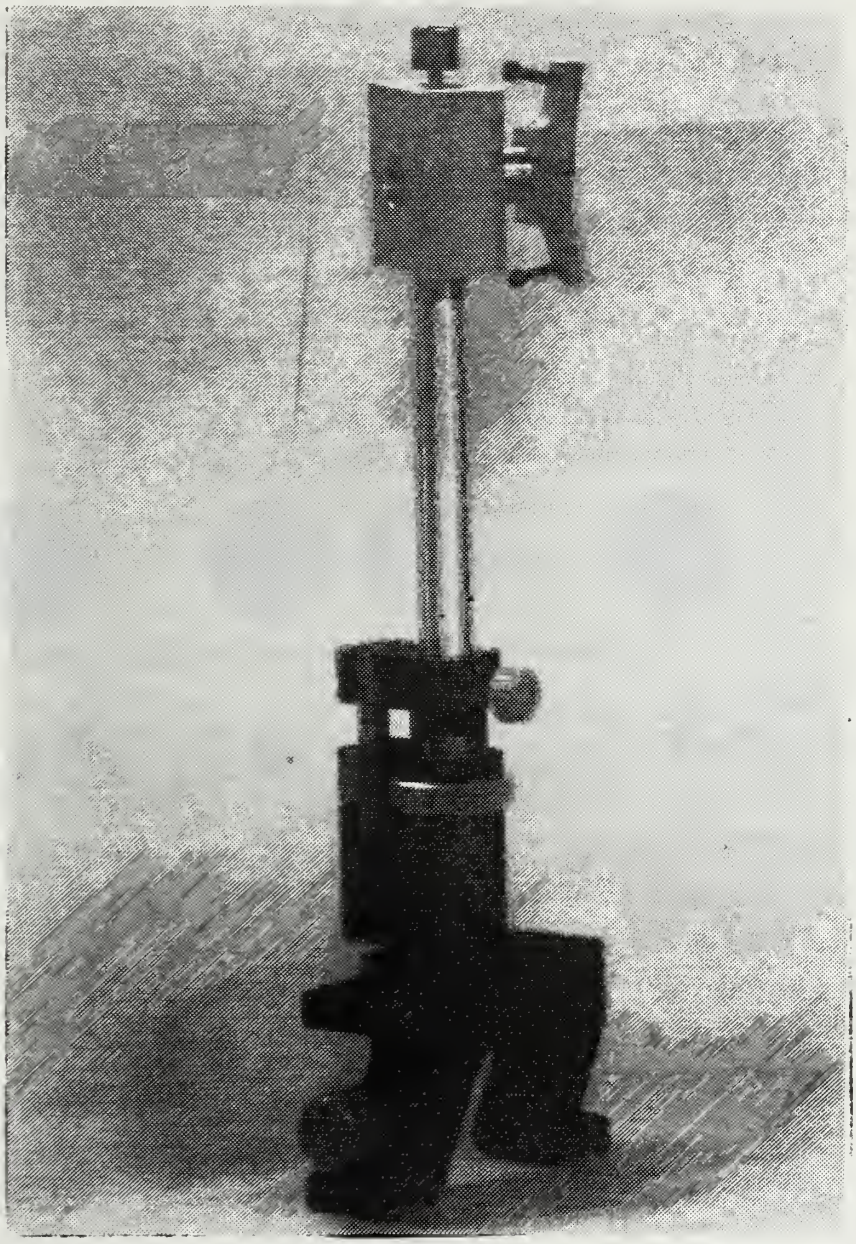

Figure A.5 Mounting leg adjustable foot combination.

7. OPTICAL RAILS AND SPACERS

Two Physitec aluminum optical rails are used to support and stablize the entire system. Three mounting feet with their corresponding leg assemblies attach to each rail. Each rail is 1.5 meters long. The two rails are held precisely parallel by a specially designed optical rail spacer installed at each end. The specific dimensions of each spacer are shown in Figure A.6 .

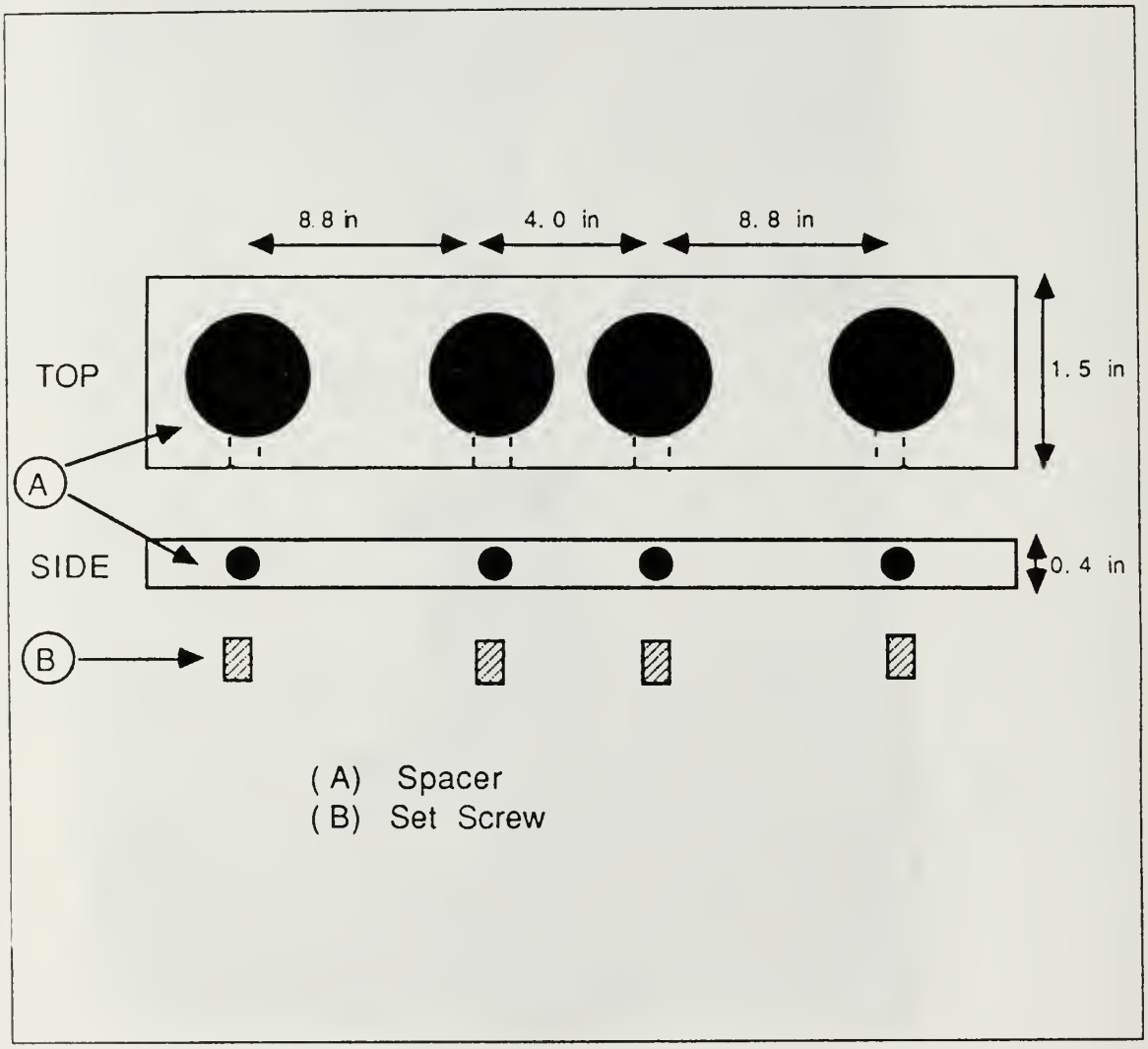

Figure A.6 Optical rail spacer.

APPENDIX B
PHOTODETECTOR BOARD

1. PHOTODETECTORS

The component used to convert photon intensity into voltage is the HAD-1100A made by EG&G Electro Optics Company. It provides the ideal combination of a silicon photodiode with good spectrical response at 632.8 nanometers with a low noise duel FET operational amplifier. The HAD-1100A is a 10 pin device with three pins connecting the photodiode section and seven pins connecting the operational amplifier section.

Information supplied from the manufacturer with the HAD-110A tells the user to connect the photodiode in the photovoltaic (zero bias) mode for low noise, low frequency (below 100 kHz) application. The He-Ne laser used in the system is considered a low frequency (near DC) source. Consequently the bias pin is grounded to allow photovoltaic operation.

The operational amplifier portion of the HAD-1100A can be connected in either the inverting or non-inverting mode. Each of the operational amplifiers on the photodetector board has been connected in the non-inverting configuration. This prevents premature amplifier burnout if an input resistance of less than 1.0 kΩ is used. NOTE: no caution about this potential hazzard is supplied by the manufacturer. Figure B.1 shows the operating circuit configuration used for each HAD-1100A. Note only nine of the ten pins are connected. Pin (5) of the device has been left disconnected to prevent any erratic response from the guard ring diode. The guard ring diode was incorporated into the HAD-1100A to improve total noise performance when an external reverse bias is applied to the photodiode. Since our application uses no external reverse bias, it is acceptable to leave it disconnected.

Each HAD-1100A is placed in a 10 pin socket to allow for quick and easy removal if necessary. The socket corresponding to pin (1) of each photodetector has white tape along its side. With pin one in place all other pins of the component will be aligned. The pin to socket scheme is shown in Figure B.2 .

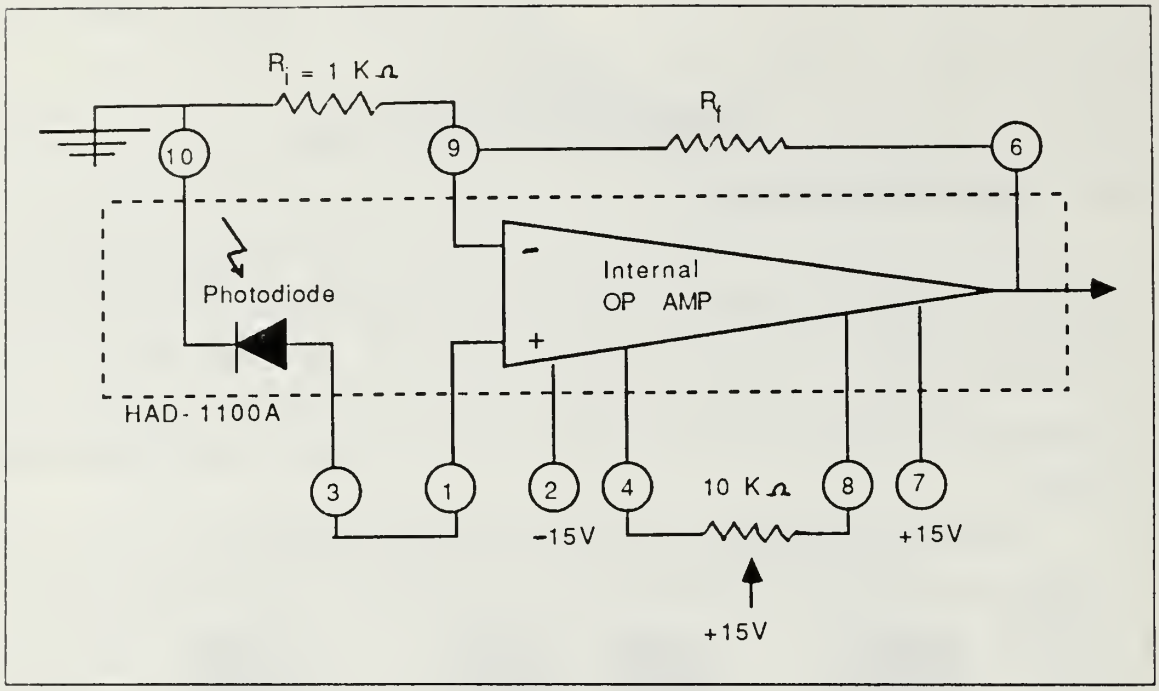

Figure B.1 HAD-1100A non-inverting mode configutation.

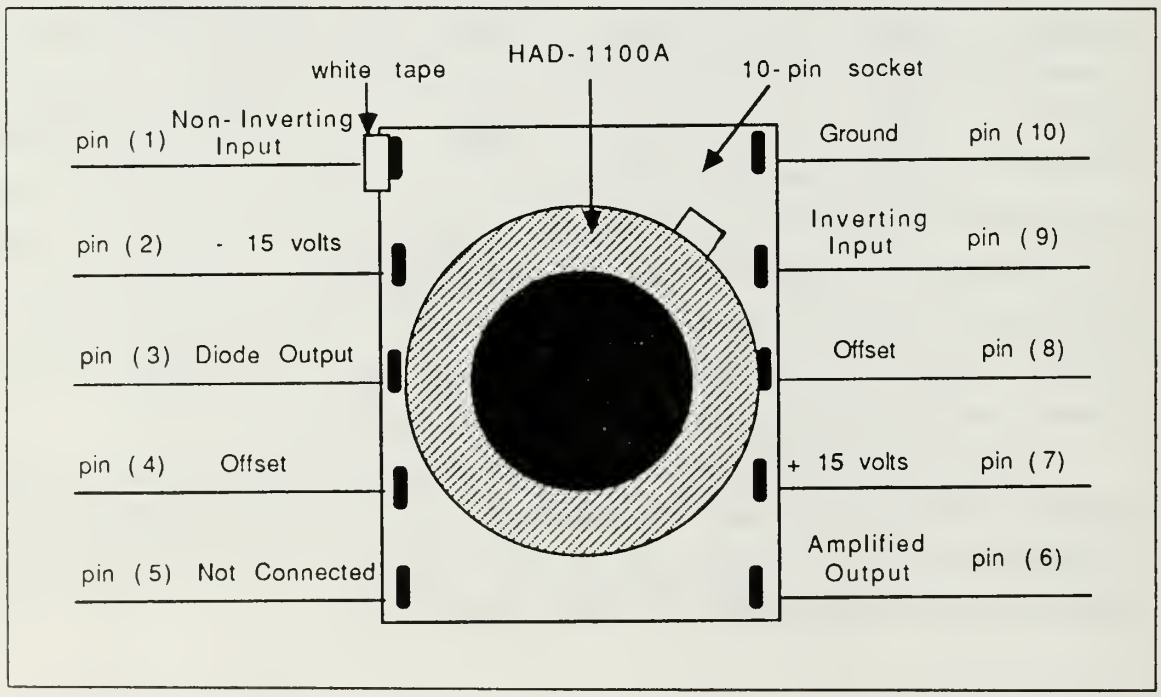

Figure B.2 HAD-1100A in a 10 pin socket.

Figure B.3 shows the physical dimensions of the HAD-1100A. The active area of the photodiode surface is 0.05 square centimeters based on the 2.54 millimeter diameter shown. Note that a tab on the outer case of the HAD-1100A indicates the location of pin (10). The price of each HAD-1100A was $76.00 .

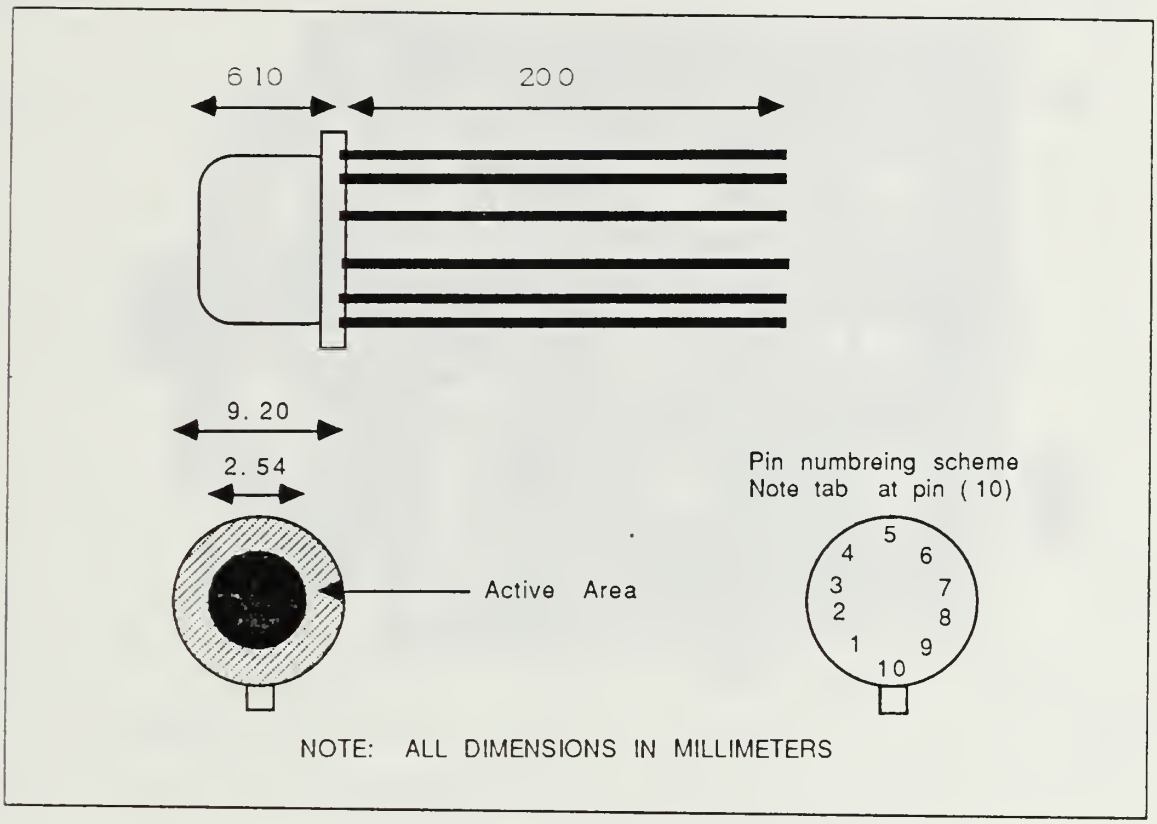

Figure B.3 HAD-1100A.

2. PHOTODIODE SPACING

Photodiode spacing is based on three criteria. First, the photodiodes should be spaced as close together as possible. Second, the spacing must allow for the physical size of the ten pin sockets that are used to mount the photodiodes onto the circuit card. Third, The distances from the optical axis to each photodiode pair should provide a ratio of $(y_2/y_1) = [2]^{1/2}$. This only simplifies the mathematical expression B.1 to B.2 .

$$D_{32} = (\lambda/0.57\pi)\,(f/y_1)\,[-\ln(I_2/I_1)/[(y_2/y_1)^2 - 1]]^{1/2} \qquad \text{(eqn B.1)}$$

$$D_{32} = (\lambda\ 0.57\pi)\ (f\ y_1)\ [-\ln(\ I_2\ I_1\ )]^{1/2} \qquad \text{(eqn B.2)}$$

Figure B.4 shows the final configuration that meets the previously mentioned criteria. The outer pair of photodiodes have off axis distances of (y_1) = 19.00 mm and (y_2) = 26.87 mm. The inner pair have off axis distances of (y_1) = 6.50 mm and (y_2) = 9.19 mm.

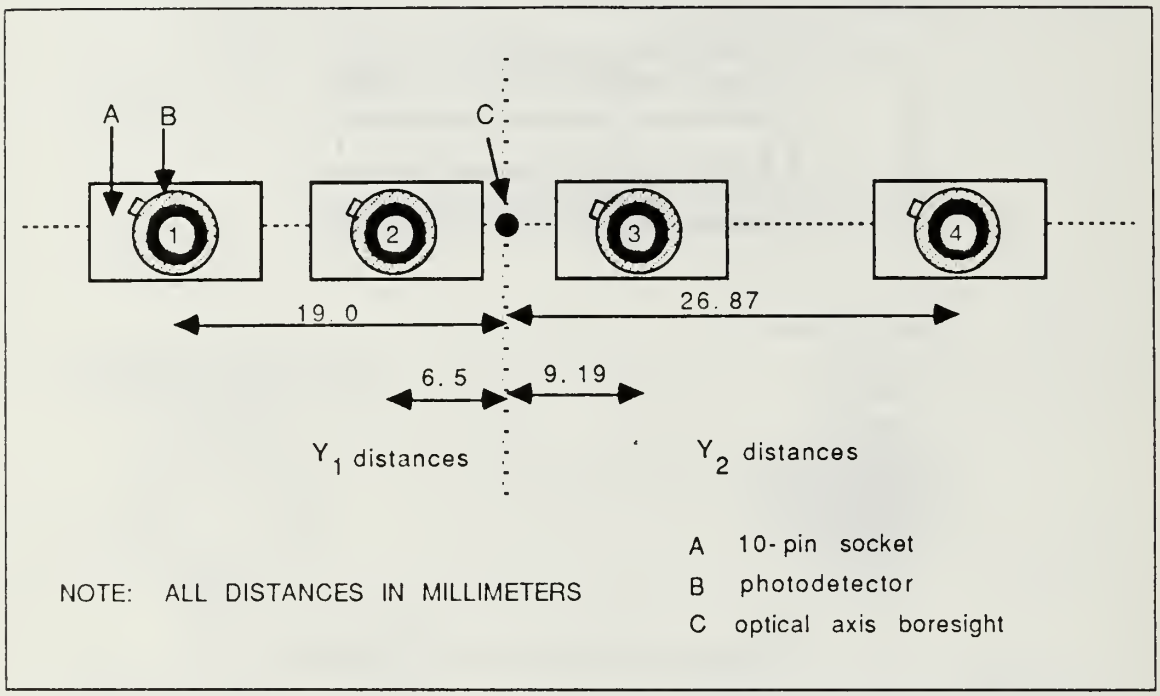

Figure B.4 Photodiode spacing configuration.

3. ELECTRICAL CIRCUITRY

Each photodetector has its own individual circuit. All four of these circuits are incorporated into a single detector board shown in Figure B.5 . The board is attached to a 22 pin edge connector for quick and easy removal. Figure B.6 is a schematic of the detector board. It shows the inputs and outputs from the board as well as the wiring color code.

The amplified outputs of photodiodes (1) and (2) can be traced along orange wires to edge pins (1) and (2) along the left side of the board. These output voltages correspond to the light intensity on a photodiode at a distance (y_1) from the optical

axis. The amplified outputs of photodiodes (3) and (4) can be traced along purple wires to edge pins (3) and (4). These output voltages correspond to the light intensity on a photodiode at a distance (y_2) from the optical axis.

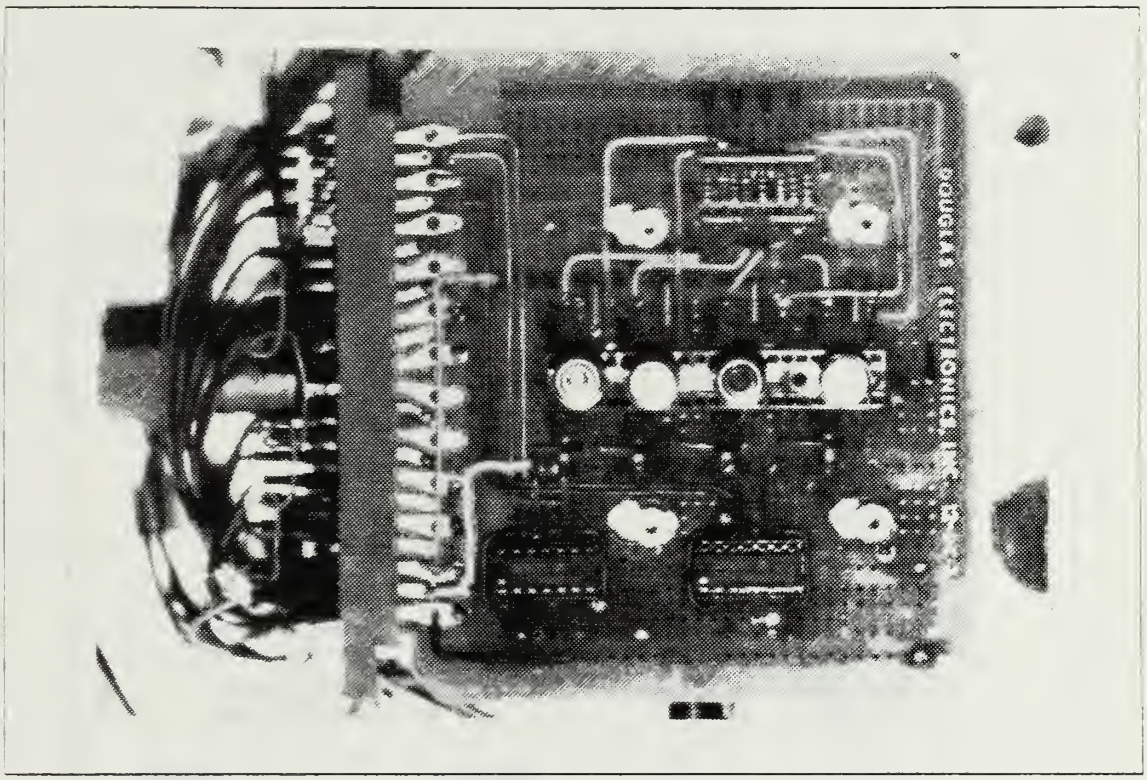

Figure B.5 Photodetector board.

All of the red wires on the board are routed to the edge pins numbered between (5) and (19). These pins are attached to the offset adjust variable resistors for each photodetector internal amplifier. The offset adjust resistors themselves are located on the photodetector external adjustment disk discribed in Appendix C.

Inputs through edge pins (20), (21) and (22) provide external power to the operational amplifiersof each HAD-1100A. In corresponding order, they are: positive 15 volts (blue wire), negative 15 volts (white wire) and reference ground (black wire).

A resistor bank on the board allows the gain of each HAD-1100A amplifier to be changed individually. All wires connecting this bank of resistors are yellow. This bank has a total of eight resistors which correspond to one pair for each photodetector. Two 747 dual operational amplifiers on the board are used to overcome induced capacitance

from output wiring associated with each detector. They are connected as non-inverting voltage followers with a gain of one.

The brown wires on the detector board which are not shown in Figure B.6 are used to test the photodiode output before it is amplified.

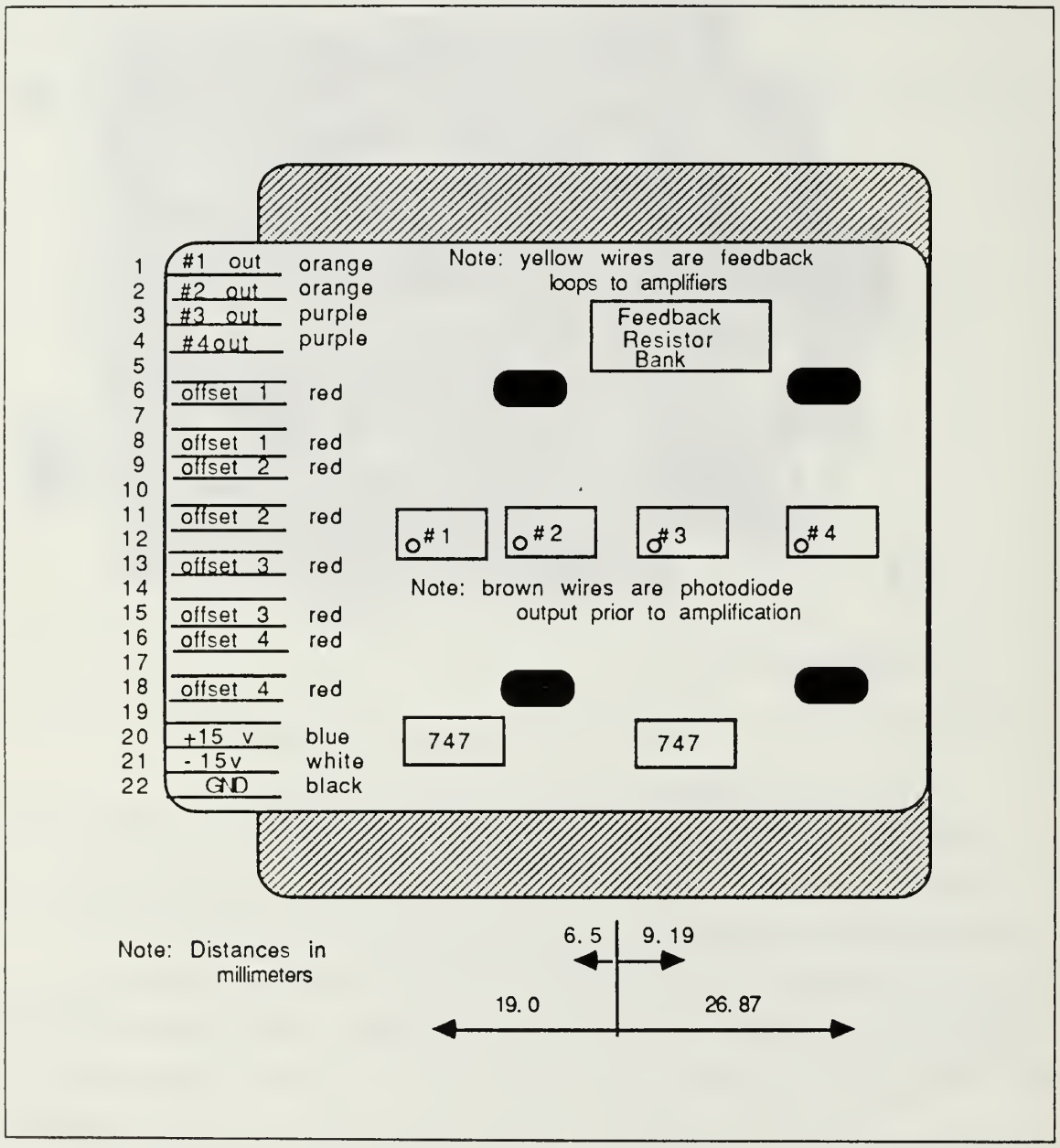

Figure B.6 Photodetector board schematic.

APPENDIX C
PHOTODETECTOR EXTERNAL ADJUSTMENT DISK

The photodetector external adjustment disk houses the photodetector selector switch, four offset control potentiometers, and four BNC jacks for monitoring photodetector outputs via oscilloscope. This disk also supports the photodetector card mounting pedistal rod. Figure C.1 shows the disk configuration.

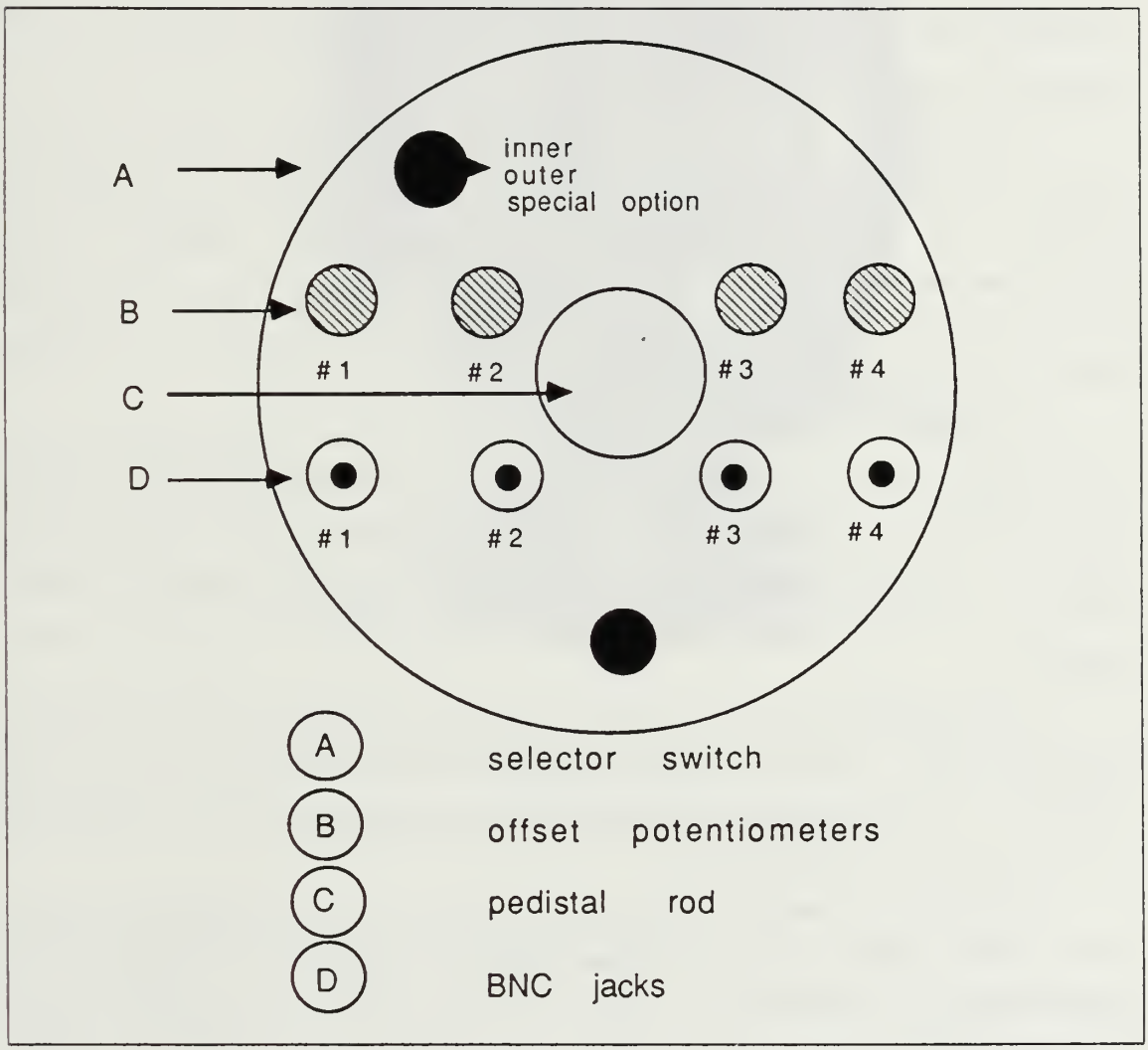

Figure C.1 Photodetector external adjustment disk.

The photodetector selector switch determines which pair of photodiodes the system uses. Selecting the inner pair will send voltages from photodetectors (2) and (3). With this position selected a (D_{32}) range from 50 microns to 266 microns can be measured. Selecting the outer pair will send voltages from photodetectors (1) and (4) to the analog computer card. With this position selected, a (D_{32}) range from 17.2 microns to 90.9 microns is available.

A third position entitled SPECIAL OPTION is available and was included as an afterthought to measure the smallest (D_{32}) sizes of which the system is capable. With this position selected, voltages from photodetectors (2) and (4) are sent to the analog computer card. Using this pair of detectors a (D_{32}) range from 12.6 microns to 32.7 microns is possible.

The four offset potentiometers are wired to their corresoponding photodetectors. They are used to establish a common reference zero for all of the HAD-1100As. This is necessary for two basic reasons. First, manufacturing differences between photodetectors can produce different conducting thresholds. Second, temperature varations (thermals) can cause the photodiodes to induce current flow even when no light source is present. These induced currents must be zeroed.

The four BNC jacks provide a means for any pair of photodetectors to be hooked up to a duel trace oscilloscope at the same time. It is desireable to monitor the photodetector output voltage noise level on an oscilloscope throughout system operation. The noise level is a key variable contributing to system error. When it becomes too large, system operation should be discontinued until the noise is eliminated.

The photodetector board pedestal rod located in the center of this disk has two functions. First, it obviously supports the photodetector board. Second, and more important, it adjusts the board's position along the optical axis so it can be positioned at the focal plane of optical lens (5).

The disk itself is made of aluminum, .500 inch thick and 9.875 inches in diameter. Three evenly spaced steel rods connect the disk securely to the optical system perpendicular to the optical axis. Figure C.2 shows a side view of the disk attached to the optical system.

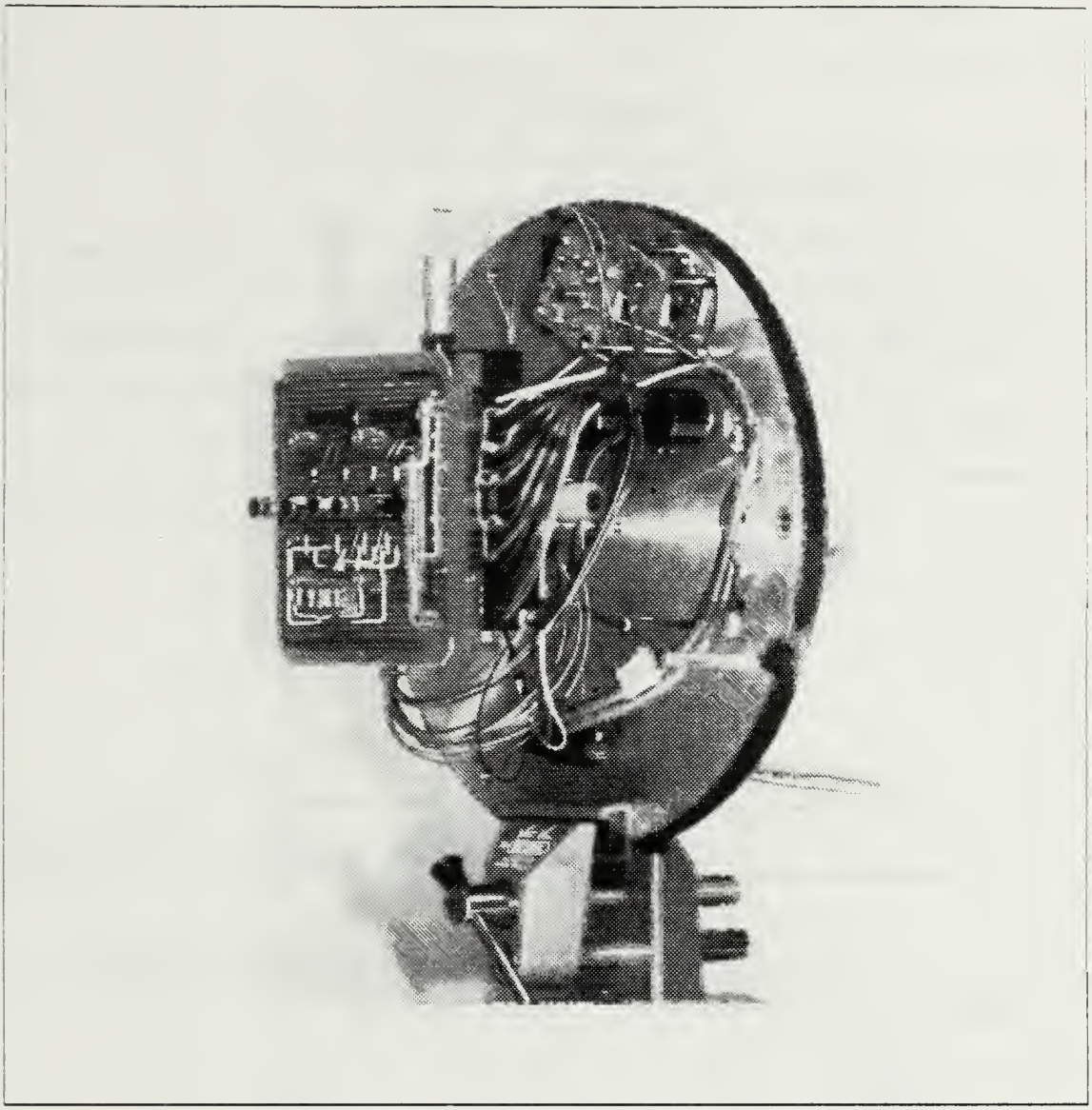

Figure C.2 Photosensor section side view.

APPENDIX D
AUTOMATIC CONTROL BOX

1. ANALOG COMPUTER CARD

At the heart of the automatic control mode is a small two chip analog computer card. This computer card lies inside the automatic control box. It is the intergal part of the feedback system and acts as a sophisticated comparator. The final output from the computer card drives the zoom lens positioning motor. Figure D.1 is the electrical circuit representation of the computer.

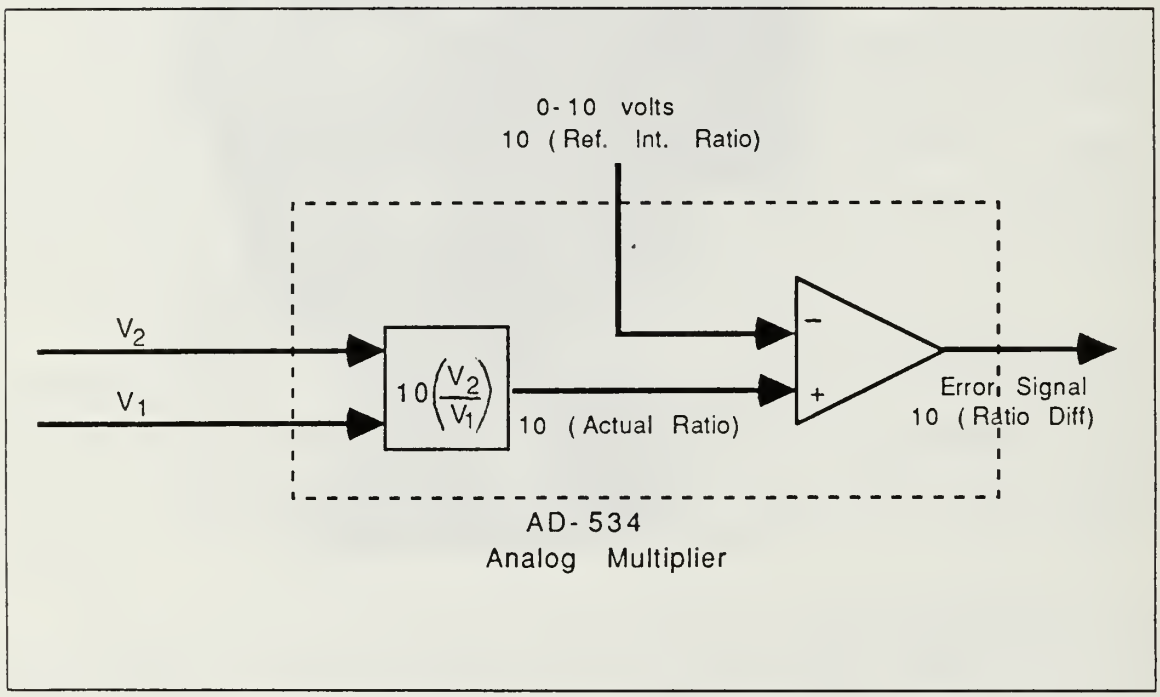

Figure D.1 Analog computer circuit.

Three inputs are given to the AD534 chip, which is an analog multiplier. The first two inputs come from the selected pair of photodetectors. They are divided into their actual intensity ratio and multiplied by 10. Their actual intensity ratio is all that is needed but the AD534 chip can not be prevented from multiplying it by 10. The third input is from the desired reference intensity ratio which also has been multiplied by 10 and entered as a negative value. The AD534 chip then compares the actual

photodetector intensity ratio (X10) with the reference intensity ratio (X10) through summation. It sends out an analog error signal which is the difference between these intensity ratios times 10.

From this point the error signal could be used to drive the positioning motor but a scheme to maintain maximum motor speed has been incorporated. This scheme calls for an amplifier with a logic circuit to turn the error signal into a plus or minus 10 volt DC signal. The speed of the positioning motor is directly proportional to the voltage it is supplied. It moves the fastest when operating at its maximum voltage limits of 10 volts DC. It stops moving entirely at its threshold of .50 volts.

A 741 operational amplifier with a variable gain from 1.0 to 100 is placed in parallel with two 10 volt zener diodes to accomplish this task. Figure D.2 shows the electrical circuit for this positioning motor preamplifier.

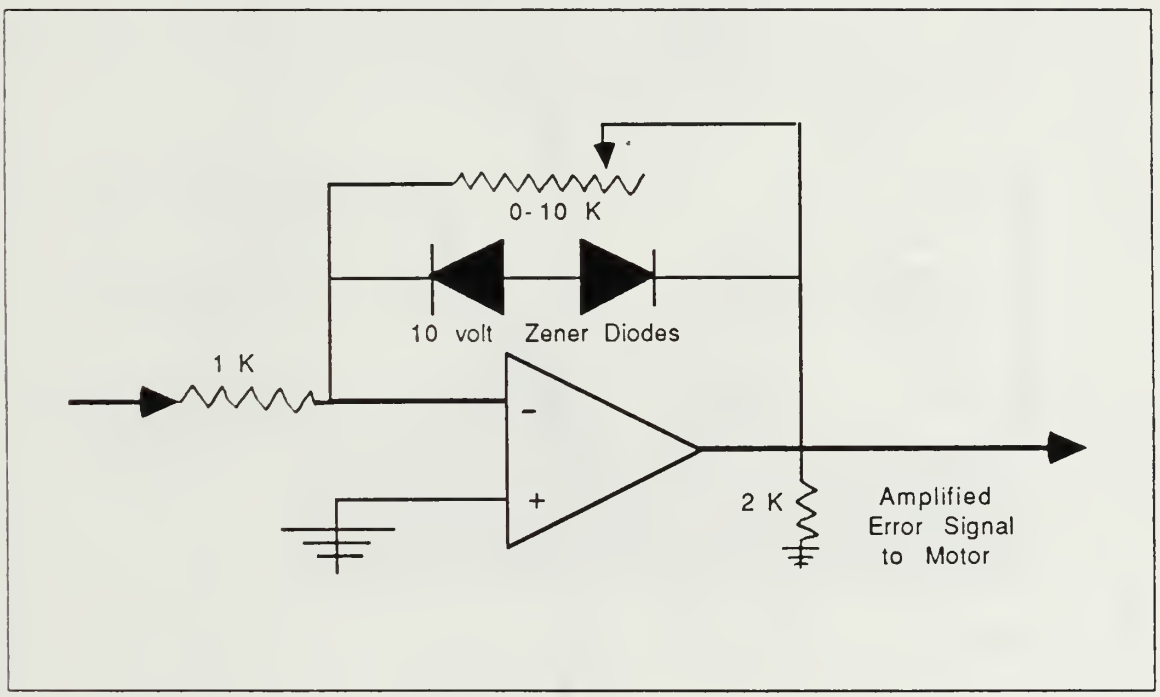

Figure D.2 Motor preamplifier circuit.

The actual gain required is determined by the desired sensitivity needed to null the motor. A gain of 62 is presently used to obtain the nulling response. A higher gain may be desired after an initial system error analysis has been conducted. Higher gains will result in reducing system error but may cause the motor to keep right on moving

through the null. Therefore one desires to set the gain as high as possible but will still allow the motor to null when the error signal is near zero. Figure D.3 shows the output response of this motor preamplifier. As the input error signal approaches zero the gain becomes important. It is desireable to have the motor stop moving when the error signal is exactly zero. The gain of the 741 establishes how close to a zero input the motor will null out. This happens when the output signal drops within plus and minus .50 volts. The slope of Figure D.3 represents this gain. As the slope becomes nearly vertical the out put signal to the motor will change too rapidly from minus 10 volts to plus 10 volts. This will result in the motor not having time to sense a .50 volt signal so it will just reverse direction without stopping. Then it will just continue to overshoot the null position back and forth. On the other hand, when the gain is too small the motor will stop prior too far away from the zero error position.

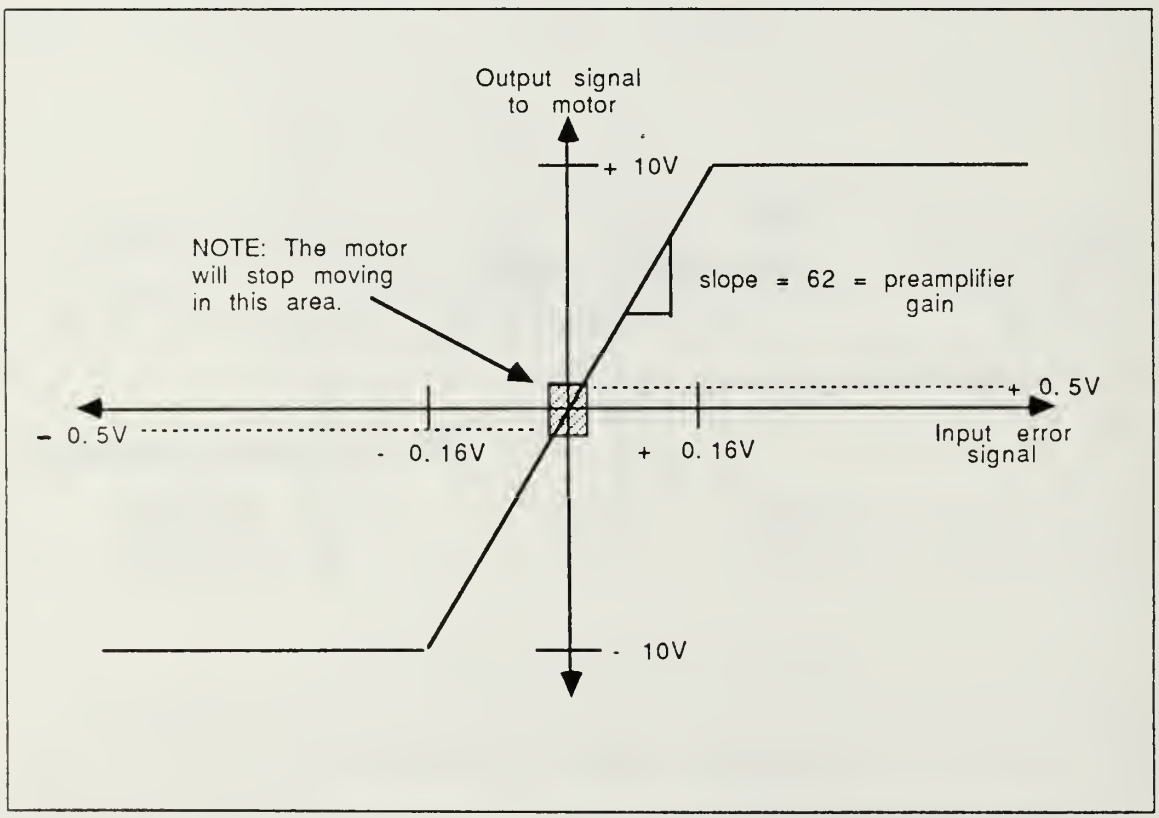

Figure D.3 Motor preamplifier logic.

A simple schematic diagram of the analog computer card is shown in Figure D.4. It shows the inputs and outputs to the board as well as the wiring color code. Note that several of the AD534 chip pins are not connected for this application.

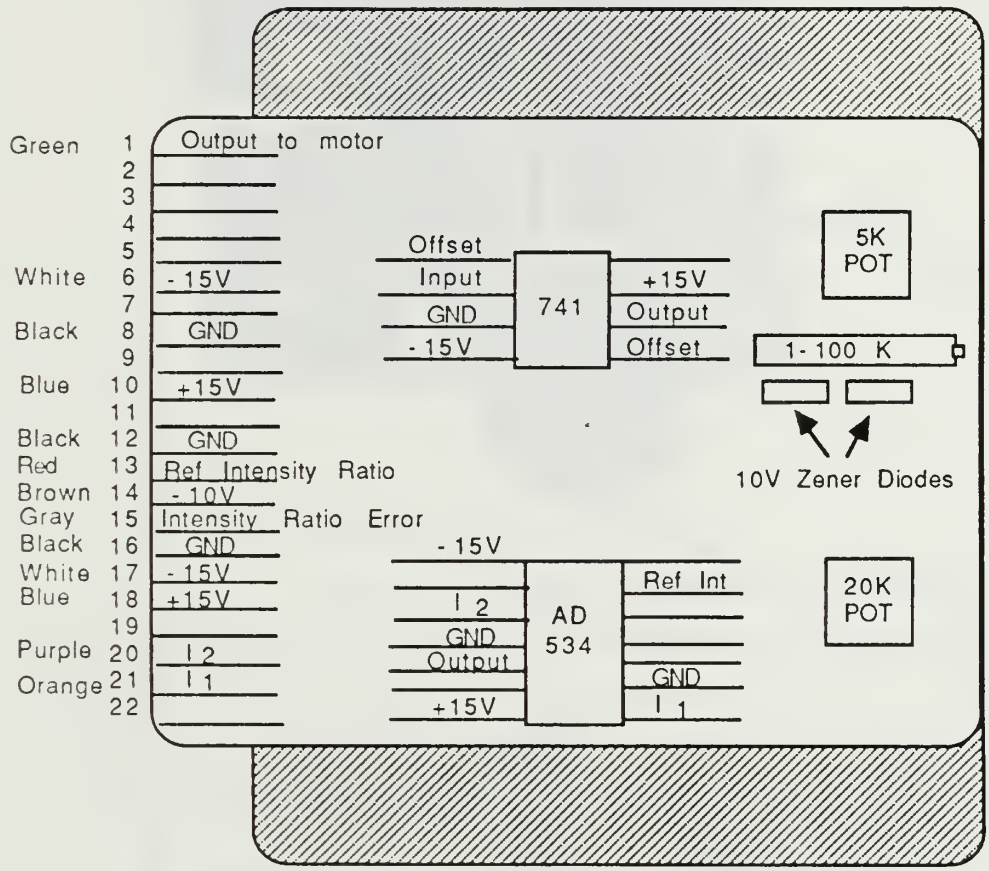

Figure D.4 Analog computer card schematic.

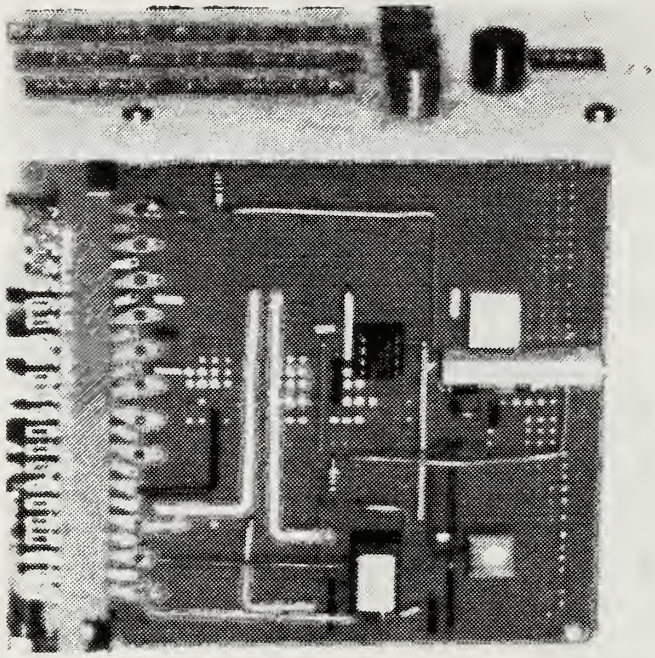

Figure D.5 Analog computer card.

2. EXTERNAL CONTROLS AND CONNECTIONS

Figure D.6 shows three faces of the automatic control box outer case as if it were unfolded. The front face has sockets for a digital voltmeter connection to monitor desired computer card signals. These signals include the reference intensity ratio times 10 (i.e. -1.0 to -10 volts), the intensity ratio error signal times 10 and the final output signal to the motor.

The top face has two controls. A ten turn potentiometer is in the center of this face to set the desired reference intensity ratio. A toggle switch is located in the corner to select automatic control or manual control operation. Selecting MANUAL allows calibration of the zoom lens positioning device and openloop operation of the entire system.

The back face has three connectors. The round connector accepts the five wire shielded cable from the photosensor section. Two 15 pin D-connectors accept the positioning motor connect cables. Figure D.7 shows the D-plug wiring configuration and Table 3 gives the automatic control box input output wiring color code.

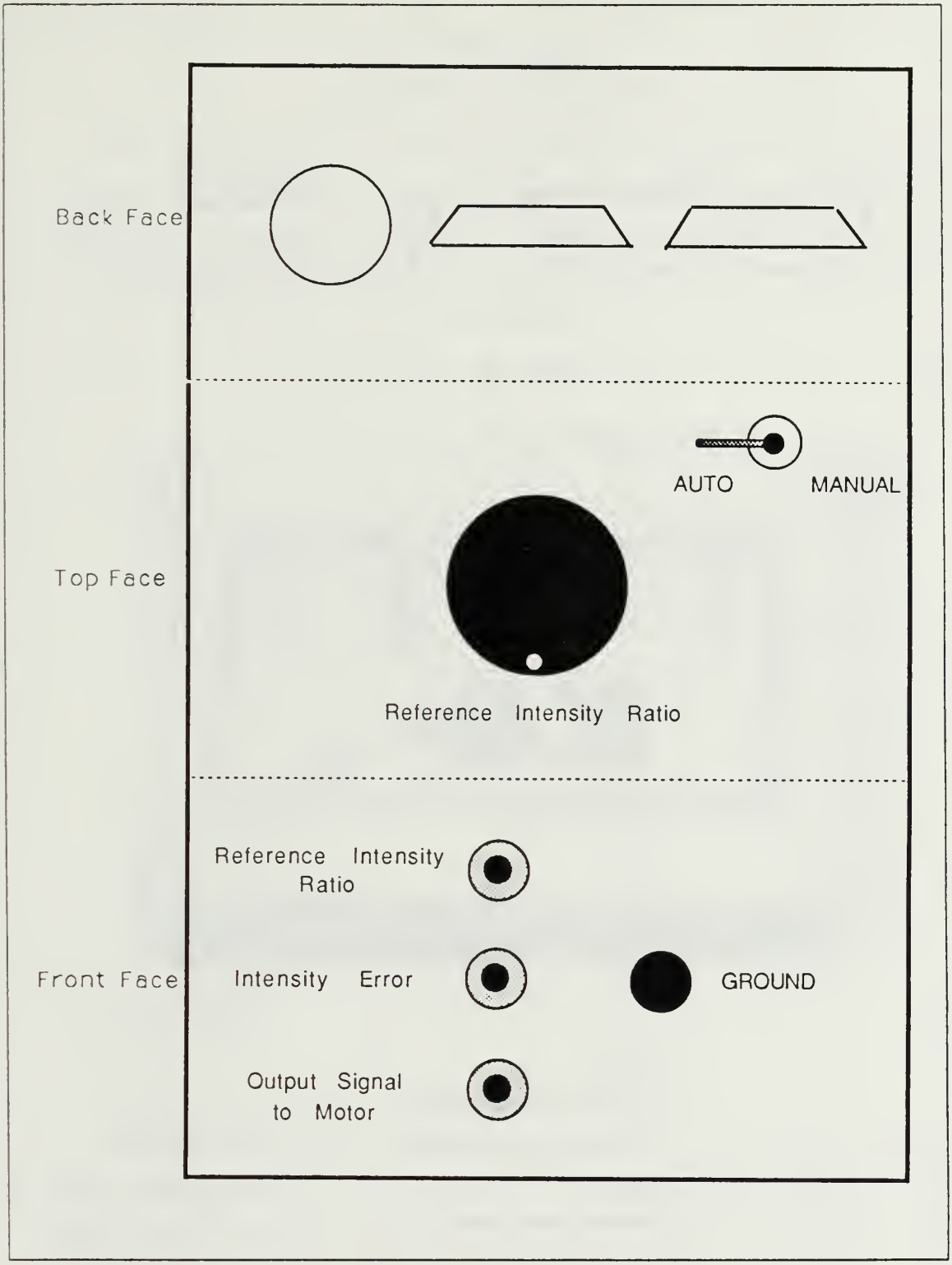

Figure D.6 Automatic control box.

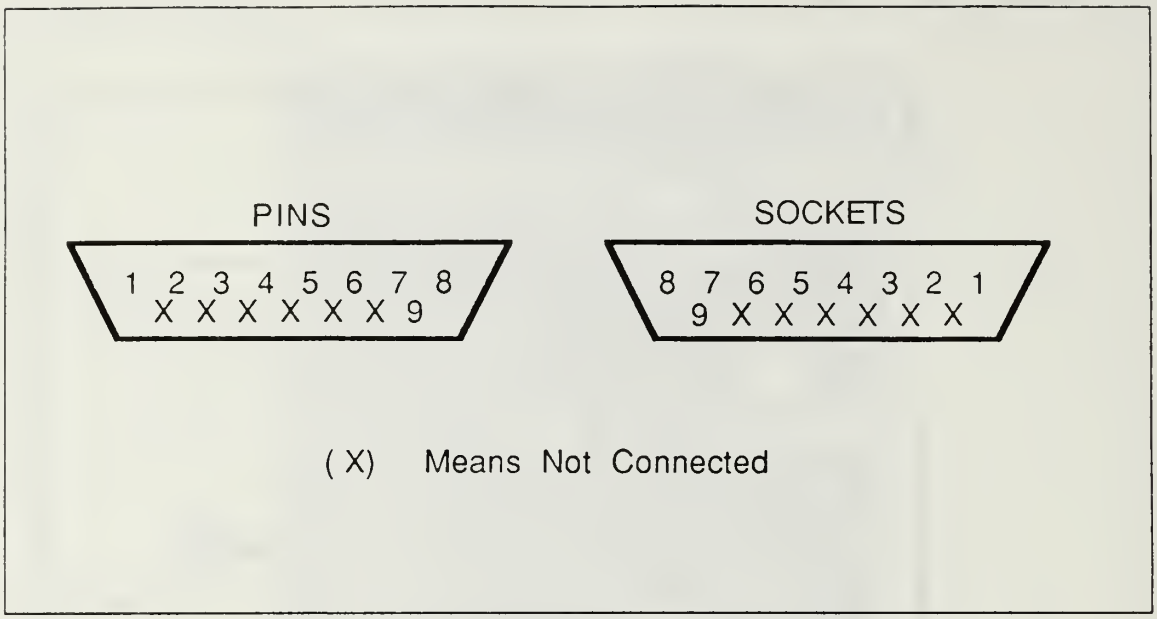

Figure D.7 15 pin D-plug configuration.

TABLE 3
WIRING COLOR CODE

Pin Number	Wire Color	Description
(1)	Blue	+ 15V DC (175mA)
(2)	Black	Analog Ground
(3)	White	- 15V DC (175mA)
(4)	Green	Command Velocity Output Signal +/- 10V DC, 20μA
(5)	Orange	Encoder Phase (1)
(6)	Orange with black stripe	Encoder Phase (2)
(7)	Black with white stripe	Analog Ground
(8)	Red	Forward Motor Limit
(9)	Red with black stripe	Reverse Motor Limit

APPENDIX E
MANUAL CONTROL BOX

The manual control box is strictly a manual controller. It can control the speed and direction of the positioning motor by slewing or jogging. It also displays the linear displacement of the motor in millimeters. This box is the standard commercial 850 CD-1 single axis controller sold by Newport Corporation and was purchased for $645.00. The manual control box is shown in Figure E.1.

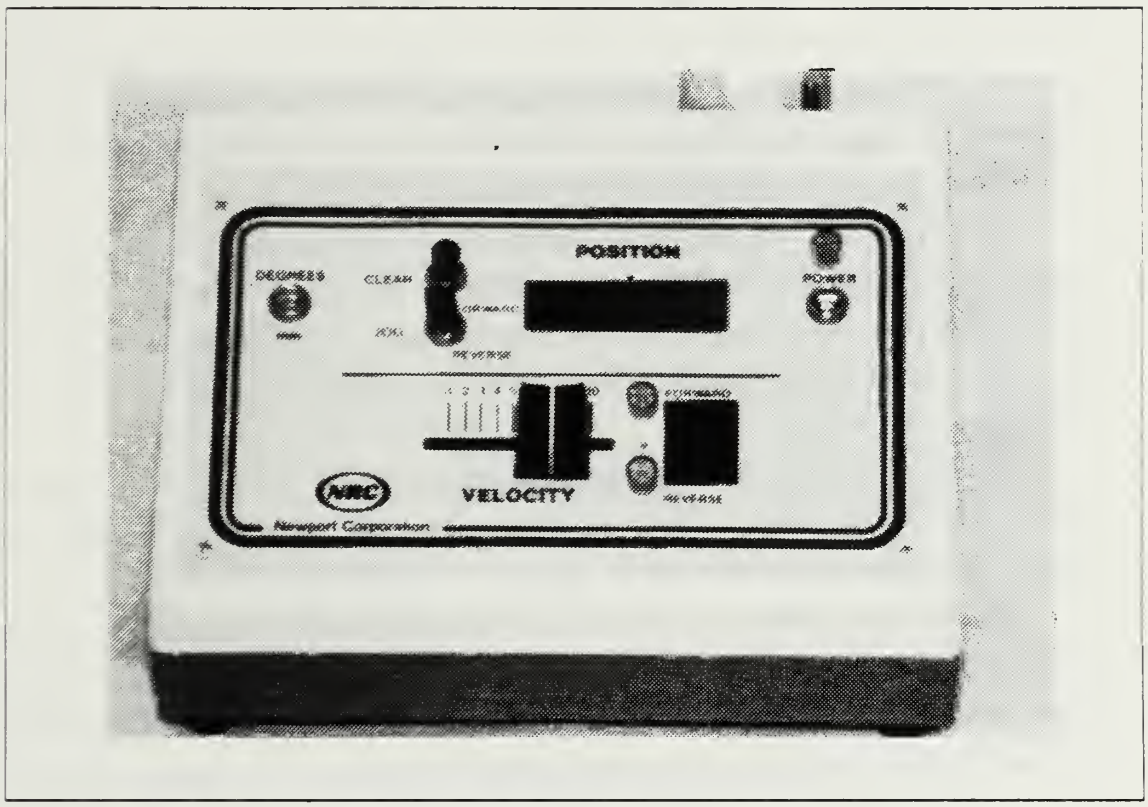

Figure E.1 Manual control box.

The power toggle switch controls power from the +/- 15V DC power supply for the entire system. When it is switched on an indicator light next to the switch illuminates. Power is then routed to the photodetector board and automatic control box as well as the manual control box.

The FORWARD REVERSE switch selects the direction of motion for the positioning motor. It simply routes a positive or negative voltage to the velocity slide lever. The velocity slide lever is attached to a variable resistor. It moves along a scale numbered from (1) to (10). This corresponds to an output signal to the motor of 1.0 to 10 volts. A 10 volt signal causes the motor to run at its fastest speed.

Two limit light indicators are on the box. They light up when the motor stalls (i.e. is prevented from moving) for a period of 35 milliseconds while a control velocity voltage is still being applied. One light comes on when forward motion has stopped. The other light illuminates when reverse motion has stopped. There are three normal conditions that can cause a limit indicator to illuminate. First, is when a physical stop is met by the motor whenever its positioning plunger rod is in the fully extended or retracted position. Second, is when the motor is unable to overcome the load it is required to position and ceases motion. Third, is when a null voltage of less than .50 volt is being sent to the motor by the automatic control box.

The jog switch can be used for minute positioning applications. It is spring-loaded to the off position. Therefore, one must continue to hold the switch in the desired direction. This sends a voltage pulse train to the motor allowing it to move slowly in minute steps (normal stepper motor operation). This feature is *not* used in normal system operation.

The last switch on the automatic control box to be mentioned is the MILLIMETER DEGREE switch. It selects the units sent to the position display window. This switch should be left in the MILLIMETER (mm) position.

The position display is a six digit LED window. It has an associated clear button to reset the display to zero. The display information is updated every five milliseconds while the positioning motor is running. The full window display gives millimeter readings down to the fourth decimal place which equates to a 0.1 micron resolution.

APPENDIX F
POSITIONING MOTOR

The zoom lens positioning motor is a high precision DC motor. It provides smooth quiet operation which is not possible in digitally driven systems. This motor is the standard commercial 850-1 motorized positioner sold by Newport Corporation and was purchased for $1170.00. The motor is 8.0 inches long with a 1.0 inch diameter. The motor with its attached velocity servo control box is shown in Figure F.1.

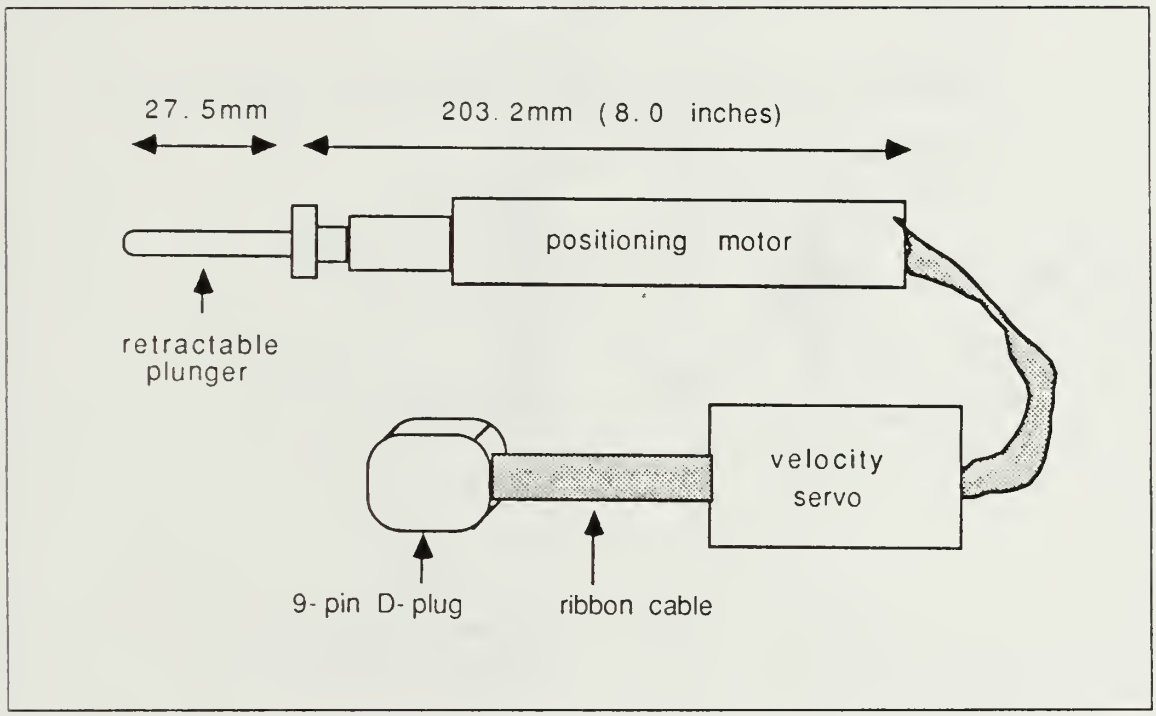

Figure F.1 Positioning motor with velocity servo control box.

In operation the DC motor/gear combination drives a lead screw which pushes a spindle plunger. The 3 16 inch diameter plunger is non-rotating and relies on an external spring force to return the plunger to its housing. The return spring presently installed in the system only exerts a 13 pound restoration load in its fully extended position. The plunger has a total travel of 27.5 mm (1.08 in.). It is this travel that is shown in the display window of the manual control box described in Appendix E. The velocity servo control box is connected to the motor by a ribbon cable as shown in

Figure F.1. Inside the velocity servo box is a bridge-type circuit that maintains a steady motor velocity despite varying external loads. This enables the positioning plunger to move in or out at a constant speed regardless of varying loads induced by the return spring.

The installed motor has a maximum linear positioning speed of .50 mm/sec in the slew mode used for normal operation. Its gearhead ratio is 262:1. A nine wire ribbon cable carries the positioning motor's input and output signals. Table 4 lists the input output pin assignments.

TABLE 4
POSITIONING MOTOR INPUT OUTPUT PIN ASSIGNMENTS

Pin Number	Description
(1)	+ 15V DC (175mA)
(2)	Analog Ground
(3)	- 15V DC (175mA)
(4)	Command Velocity Output Signal + - 10V DC, 20μA
(5)	Encoder Phase (1)
(6)	Encoder Phase (2)
(7)	Analog Ground
(8)	Forward Motor Limit
(9)	Reverse Motor Limit

The motor is attached to the system with a specially designed mounting flange that allows the motor to be easlily repositioned by sliding its body forward or backward. This is neccessary to make full use of the zoom lens travel which is 2.5 millimeters greater than that of the motor's positioning plunger. The special mounting flange designed for the motor is shown in Figure F.2.

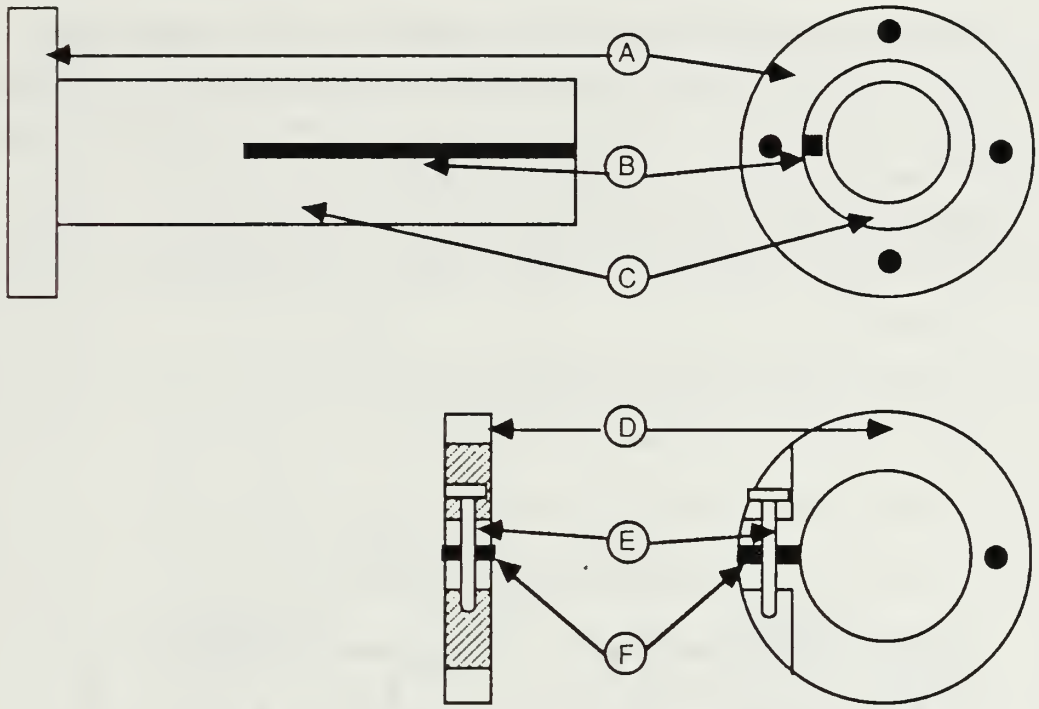

(A) Flange
(B) Sleeve
(C) Slit
(D) End Clamp
(E) Tightening Screw
(F) Slit

Figure F.2 Positioning motor mounting flange.

APPENDIX G
RIBBON INTERCONNECT CABLES

The interconnect cables are general purpose nine wire ribbon cables. These cables are unshielded. They are used for interconnecting all external modules (i.e. auto control box, manual control box and velocity servo control box) to the zoom lens positioning motor.

These cables have standard subminiture 9-pin D-connectors which have blue covers and 15-pin D-connectors with white covers. The pin numbering schemes are shown in Figure G.1.

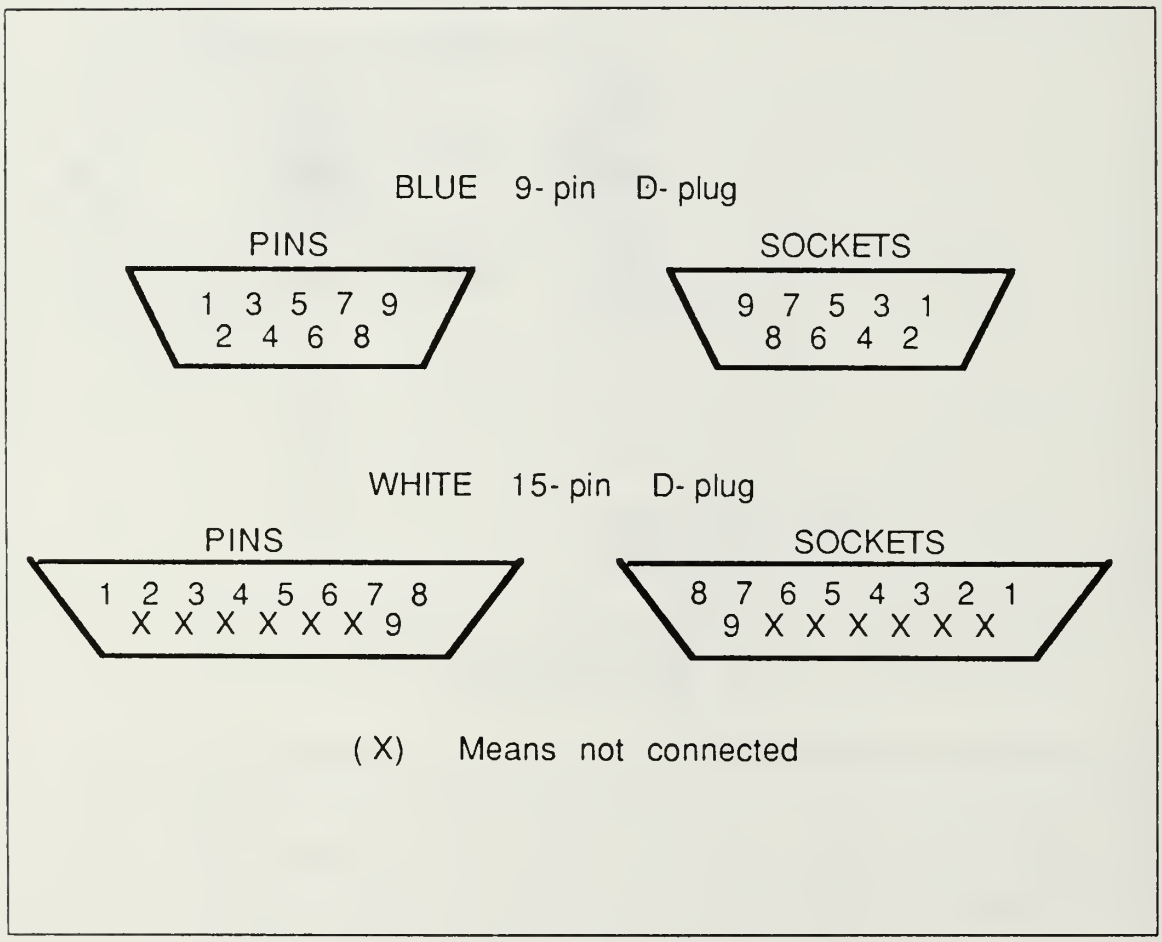

Figure G.1 Ribbon cable connector pin numbering schemes.

APPENDIX H
ALIGNMENT AND OPERATING PROCEDURES

Current work with the system has resulted in several lessons learned relating to the order in which one should align and operate the device. The following procedure is suggested for system alignment:

- step 1 Remove all optical and photodetector shielding. (The red covers)
- step 2 Remove (or cover up) all photodetectors on the photodetector board. (This prevents damage should direct laser light be inadvertently focused on them.)
- step 3 Turn on the laser.
- step 4 Level the laser with a small liquid level. (A small liquid level needs to be placed on the black diffuser tube for this step)
- step 5 Vertically raise the laser until the laser beam touches the optical system gun sights.
- step 6 Horizontally adjust the laser until the laser beam passes through the optical gun sights.
- step 7 Vertically lower the laser until the laser beam is centered on the first objective lens.
- step 8 Adjust the first objective lens fore and aft until the laser beam reaches its minimum spot size at the center block on the first beamstop.
- step 9 Remove the center block on the first beamstop. (This allows direct laser light to pass through to the photodetector board.)
- step 10 Push the photodetector board forward until the laser beam reaches its minimum spot size on the board.
- step 11 Operate the positioning motor in the MANUAL MODE to move the zoom lens in and out while monitoring the location of the laser spot on the photodetector board. (The laser spot should remain in a fixed location. If it moves horizontally or vertically with zoom lens travel, then adjustments have to be made to the rear mounting legs.)
- step 12 Adjust the photodetector board horizontally and vertically. (This should be done until the laser spot is boresighted on the center cross-hairs on the board. THE SYSTEM IS NOW OPTICALLY ALIGNED.)
- step 13 Reinstall the center block over the center of the first beamstop slit. (This cuts off direct laser light to the photodetector board.)
- step 14 Install (or uncover) the four HAD-1100As on the photodetector board. (NOTE: Pin (1) of each HAD-1100A should be placed into the socket with white tape on its side.)
- step 15 Pull the photodetector board back 1.0-centimeter with the adjustment rod. (This allows the photodetectors to be positioned at the rear focal plane of lens five.)
- step 16 Reinstall the optical and photodetector system shielding. (The red covers)

The following procedure is suggested for system operation:

- step 1 Ensure the system is aligned.
- step 2 Ensure the optical and photodetector shielding is installed. (The red covers.)
- step 3 Turn on the laser.
- step 4 Set the AUTO MANUAL switch on the automatic control box to MANUAL.
- step 5 Set the ON OFF switch on the manual control box to ON.
- step 6 Check each photodiode output with the oscilliscope and adjust each output to zero with the corresponding offset control knob.
- step 7 Select the appropriate pair of photodetectors. (INNER for 50μm - 266μm, OUTER for 17μm - 90μm and SPECIAL OPTION, which uses photodetector (2) and (4), for 12.6μm - 32.7μm)
- step 8 Connect the appropriate photodetector outputs to the oscilliscope and select the (ALT) position on the scope to display both voltages simutaineously.
- step 9 Connect a digital multimeter to the automatic control box with the (0 to 20) volt range selected.
- step 10 Input the desired optimum reference intensity ratio into the automatic box. (NOTE: A range of 0.50 to 0.80 optimum intensity ratio is desired and depends on the size particles to be measured. This range will be read out on the digital meter as a range of -5.0 to -8.0 volts.)
- step 11 Calibrate the optical lens position with the readout on the manual control box by running the zoom lens to zero travel manually and seting the readout to zero.
- step 12 Reposition the zoom lens manually to its mid-travel position. (This step allows the system to search in either direction in minimum time when AUTO MODE is selected.)
- step 13 Release the particles to be measured into the test section.
- step 14 Select AUTO on the automatic control box. (The system will now search for the correct lens position for the corresponding particle size.)
- step 15 Monitor the "yellow" limit lights on the manual control box until either one illuminates. (This indicates the motor has stopped.)
- step 16 Select MANUAL on the automatic control box. (This locks in the position on the manual control box display.)
- step 17 Record the zoom lens position from the digital display on the manual control box. (Enter the system focal length chart (Appendix A) with this position to determine the corresponding system focal length.)
- step 18 Determine particle size (D_{32}) by multiplying the system focal length by the appropriate proportionality factor (k).

$k_{inner} = 54.366 \times (10)^{-6} [-\ln(\text{Ref intensity ratio})]^{1/2}$

$k_{outer} = 18.599 \times (10)^{-6} [-\ln(\text{Ref intensity ratio})]^{1/2}$

$k_{special\ option} = 54.366 \times (10)^{-6} [-\ln(\text{Ref intensity ratio} / 16.1)]^{1/2}$

LIST OF REFERENCES

1. Van deHulst, H. C., *Light Scattering by Small Particles*, John Wiley and Sons, Inc., 1957.

2. Shavit, Z., *Measurements and Designs Related to Electrical Spray Modification in a T-56 Combustor*, Contractor Report NPS 67-85-012CR, Naval Postgraduate School, Monterey, CA, December 1985.

3. NASA Technical Paper 2156, *Particle Sizing by Measurement of Forward-Scattered Light at Two Angles* by D. R. Buchelle, 1983.

4. Powers, John, *Particle Sizing From Forward Scattered Light at Two Angles Using a Variable-Focal-Length Optical System*, M.S.Ae Thesis, Naval Postgraduate School, Monterey, CA, December 1984.

INITIAL DISTRIBUTION LIST

		No. Copies
1.	Defense Technical Information Center Cameron Station Alexandria, VA 22304-6145	2
2.	Library, Code 0142 Naval Postgraduate School Monterey, CA 93943-5002	2
3.	Chairman, Code 67 Department of Aeronautics Naval Postgraduate School Monterey, CA 93943	1
4.	Professor O. Biblarz, Code 67Bi Department of Aeronautics Naval Postgraduate School Monterey, CA 93943	5
5.	Professor R. Partelow, Code 62Pw Department of Electrical Engineering Naval Postgraduate School Monterey, CA 93943	1
6.	Professor J. Miller, Code 67Mo Department of Aeronautics Naval Postgraduate School Monterey, CA 93943	1
7.	LCDR Ludwig August Kern 747 Sherman Ave Oconomowoc, WI 53066	2
8.	Dr. A. T. Kelly Dept. of Mechanical and Aerospace Engineering Princeton University Princeton, NJ 08544	1
9.	Commanding Officer Naval Air Systems Command Attn: Mr. G. Derderian, Code AIR 330B Washington, D.C. 20361	1
10.	Commanding Officer Naval Air Systems Command Attn: Mr. T. Momiyama, Code AIR 330 Washington, D.C. 20361	1
11.	Mr. C. D. B. Curry, ONR Patent Council Naval Station, Treasure Island Bldg 7, Room 82 San Francisco, CA 94130	2
12.	Mr. Zeev Shavit c o Professor O. Biblarz, Code 67Bi Department of Aeronautics Naval Postgraduate School Monterey, CA 93943	1

13. LCDR J. Powers
c o Professor O. Biblarz, Code 67Bi
Department of Aeronautics
Naval Postgraduate School
Monterey, CA 93943 1

Thesis
K38735 Kern
c.1 Prototype particle size anlyzer incorporating variable focal length optics.